symmetry

MDPI

Article

New Approach to Cross-Correlation Reflectometry Diagnostics of Nonlocality of Plasma Turbulence

Alexander B. Kukushkin [1,2,3,*] and Andrei A. Kulichenko [1]

[1] National Research Center "Kurchatov Institute", 123182 Moscow, Russia; kulichenko_aa@nrcki.ru
[2] National Research Nuclear University MEPhI (Moscow Engineering Physics Institute), 115409 Moscow, Russia
[3] Moscow Institute of Physics and Technology, National Research University, 141700 Dolgoprudny, Russia
* Correspondence: kukushkin_ab@nrcki.ru

Abstract: One of the most important properties of stochastic nonlinear processes, including the turbulence of the hydrodynamic motion of continuous media, is distant spatial correlations. To describe them, an approach was proposed by Shlesinger and colleagues based on a linear integro-differential equation with a slowly decaying kernel, which corresponds to superdiffusion (nonlocal) transfer in the regime of Lévy walks (Lévy flights when the finite velocity of the carriers is taken into account). In this paper, we formulate a similar approach that makes it possible to formulate the problem of determining these properties from the scattering spectra of electromagnetic (EM) waves and cross-correlation reflectometry. A universal description of the relationship between the observed symmetric quasi-coherent component in the spectrum of scattered EM waves in plasmas and a process of the Mandelstam–Brillouin scattering type is obtained. It is shown that the nonlocality of spatial correlations of density fluctuations in a turbulent medium is due to long-free-path carriers of the medium's perturbations, for which the free path distribution function is described by the Lévy distribution. The effectiveness of the proposed method is shown by the example of the interpretation of the data of cross-correlation reflectometry of EM waves in the radio-frequency range for the diagnosis of turbulent plasma in magnetic confinement devices for axisymmetric toroidal thermonuclear plasma.

Keywords: cross-correlation reflectometry; superdiffusion; Biberman–Holstein equation; Lévy walk; Mandelstam–Brillouin scattering

check for updates

Citation: Kukushkin, A.B.; Kulichenko, A.A. New Approach to Cross-Correlation Reflectometry Diagnostics of Nonlocality of Plasma Turbulence. *Symmetry* **2022**, *14*, 1265. https://doi.org/10.3390/sym14061265

Academic Editors: Markus Büscher and Sam Vinko

Received: 1 May 2022
Accepted: 13 June 2022
Published: 19 June 2022

1. Introduction

One of the most important problems of diagnostics and control of magnetically confined plasma in devices for controlled thermonuclear fusion is the measurement of the spatial distribution of the plasma density and the main characteristics of its density fluctuations. The latter play an important role in confining the thermal energy of the plasma and the possibility of maintaining thermonuclear fusion in high-temperature plasma. The most effective diagnostics of the main characteristics of plasma density fluctuations are active diagnostics based on the injection of electromagnetic (EM) waves into the plasma in the electron cyclotron frequency range and the injection of beams of heavy ions (heavy ion beam probing) and hydrogen atoms (beam emission spectroscopy). This work is devoted to the development and application of the theory of diagnostics of nonlocal properties of plasma density fluctuations using diagnostics of the first type—plasma reflectometry by EM waves. The nonlocal properties of plasma density fluctuations are of particular practical interest due to the importance of the observed nonlocal properties of heat transfer in thermonuclear plasmas. The developed methods for analyzing the nonlocal properties of plasma density fluctuations so far have been based on approaches in which plasma fluctuations are described in terms of models based either on a priori assumptions of a general nature or on simplified approaches not based on solving kinetic equations. Therefore, the task of formalizing models within the framework of more general and more rigorous approaches remains relevant.

In this paper, we present a theoretical model of density fluctuations in a medium with stochastic nonlinear processes, which also covers the case of turbulent plasma. Accounting for the nonlinearity of processes lies in the assumption of the existence of long-lived fluctuations of the plasma density (on a qualitative level, this can be illustrated by the possible existence of solitary waves: for example, two-dimensional solitons described by the well-known Kadomtsev–Petviashvili equation). The kinetic model of a turbulent medium makes it possible to describe the dynamics of a statistical ensemble of localized density perturbation carriers (localized density fluctuations), which can be considered in a linear approximation, taking into account such processes as (a) the birth of carriers from the thermal energy of the plasma, (b) the reverse process of their disappearance, (c) motion in a plasma with a finite free path, and (d) stoppage of the carrier without its disappearance (capture) and resumption of motion. In this case, the phenomenologically introduced parameters of these processes are subject to restoration by a comparison with experimental data on the fine spectral characteristics of the scattering of the probing EM in plasma.

The theoretical model proposed by us is used to describe the cross-correlation reflectometry of nonlocality in a turbulent plasma. The proposed model generalizes the previously developed models in that the spectral characteristics of the signals of such reflectometry are obtained by solving the kinetic equation for the space–time dynamics of plasma density fluctuations and take into account phenomena that have not been covered by existing models. First of all, the property of significant dispersion of the distribution of medium perturbation carriers over their free path length is taken into account, which is precisely the generator of nonlocality (superdiffusion) of perturbation transfer. Next, we briefly explain the specifics of nonlocality in transfer processes and the status of the theory of such processes.

Normal (ordinary) diffusion is defined as Brownian motion and is described by a Fokker–Planck type differential equation. The Green's function of such an equation, which describes the propagation of a disturbance from a point instantaneous source in a homogeneous stationary medium, is a Gaussian with an argument that determines the front propagation law $r_{fr}(t) \sim (Dt)^{\beta}$, where $\beta = 1/2$ and D is the diffusion coefficient. However, this law is violated for a wide class of physical processes, where the free path distribution function, the so-called step-length probability density function (PDF), for the carriers of the medium disturbance turns out to be slowly decreasing with increasing distance, namely in a power-law manner, and not exponentially. This leads to the divergence of the diffusion coefficient, which is formally determined in the form of the dispersion of the PDF, and the calculation of the above law of front propagation from the results of the analysis of the corresponding Green's function gives $\beta > 1/2$. This type of transfer is called superdiffusion or nonlocal.

Superdiffusion transport, as well as the concept of Lévy flights associated with it, introduced by Mandelbrot [1,2] (see p. IX in monograph [2] and reviews [3–5]), covers many phenomena in physics and other disciplines. The model of nonlocal transfer, called "Lévy walk with stops" (see [6–8] and review [9]), is relevant for such problems as the transfer of resonant radiation in astrophysical gases and plasmas [10–13], biological migration (Section 6 in [9]), and energy transfer by linear waves in plasmas [14].

Analytical methods are well developed for problems of stationary nonlocal transfer, such as, for example, the theory of resonant radiation transfer with complete frequency redistribution in the act of absorption and emission of a photon by an atom or ion in a gas or plasma [15–27]. For more complex problems, namely nonstationary nonlocal transport, a method for calculating the characteristics of nonlocal transport of interest (primarily an approximate description of the Green's function characterizing the dynamics of the propagation front of the perturbation of a medium from an instantaneous point source) was developed in [28] in the limit of infinite speed of light and generalized to the case taking into account the delay (i.e., the finite speed of light) in [29–32]; see also review [33]. This method for describing nonstationary superdiffusion processes is applied in this work to describe the kinetics of moving density fluctuations in a turbulent medium. This made it possible to formulate an algorithm for reconstructing the nonlocal properties of stochastic processes in a medium from the spectrum of its density fluctuations, which is diagnosed from the scattering spectra of EM waves in the medium.

The developed approach is based on the use of the concept of Lévy walks (Lévy flights taking into account the finite speed of carriers). Such a concept was proposed in [34] for stochastic nonlinear processes, including the turbulence of the hydrodynamic motion of continuous media. The description of distant spatial correlations was based on a linear integral–differential equation with a slowly falling kernel, which corresponds to superdiffusion (nonlocal) transport in the Lévy walk mode. The similarity laws obtained in [34] made it possible to qualitatively establish a relationship with the Richardson law [35] for the motion of the perturbation front in a hydrodynamic turbulent medium and the Kolmogorov spectrum [36] for uniform stationary turbulence. In this paper, we formulate a fundamentally close approach based on the concept of Lévy walks, albeit within a different physical and mathematical model.

In the problem of correlation reflectometry of turbulent plasma of interest to us, the phenomenon of nonlocality (superdiffusion) of heat and particle transfer processes is widely studied in relation to this and other plasma diagnostics (see, for example, monograph [37]). The models used to describe plasma density fluctuations vary over a wide range. Let us explain this by the example of the radial Doppler correlation reflectometry of the tokamak plasma, which is of interest to us. The pair correlation function of the plasma density can be chosen from general statistical considerations as a time-independent function with a Gaussian or power-law dependence on the coordinate difference: see, for example, (21) in [38], where using the general approach [39], the expected signal of cross-correlation reflectometry was calculated taking into account the volumetric scattering of the probing wave. Another model is the representation of a turbulent field of density fluctuations as a finite set of fluctuations with given kinematic parameters of individual perturbations—lifetime, motion velocity, and mean free path (see, for example, the formula on p. 449 in [40]). Our goal is to obtain an analytical representation of the density of fluctuations in a turbulent plasma, in which the free path and the velocity of motion are given by a distribution with dispersion and not just by the average value. In this case, the analytical description of density fluctuations itself is not an a priori given function but a solution to a kinetic equation that takes into account elementary mechanical processes in the dynamics of individual density perturbations.

The specific practical goal of this work is to apply the obtained theoretical results to the interpretation of the data of correlation reflectometry of EM waves in the radio frequency range for diagnosing turbulent plasma in tokamaks. Of particular interest is the analysis of a phenomenon discovered at the T-10 tokamak and called "quasi-coherent oscillations" [41–43] (in international terminology, quasi-coherent mode). Subsequently, the same results were obtained on other tokamaks using the same diagnostics-reflectometry (TEXTOR, ToreSupra, KSTAR, HL-2A, and J-TEXT tokamaks). In addition, the spectrum with quasi-coherent components was also observed with the help of another diagnostic—heavy ion beam injection (see, e.g., review [44]) on the same T-10 tokamak (the results of these diagnostics are compared in [45]). If the observed symmetric peaks (relative to the frequency of diagnostic probing radiation) in the scattering spectrum on density fluctuations are the result of the presence of a distinguished velocity of their motion relative to the plasma, then we have an analogue of the fine structure of Mandelstam–Brillouin scattering. Such a structure was theoretically predicted for the scattering of light by sound waves in elastic media, including liquids, amorphous media, and solids (see the paragraph "Rayleigh scattering in gases and liquids" in [46]). The reason for the appearance of a fine structure in the spectrum of scattered radiation (i.e., the "splitting" of an almost monochromatic line, which is the spectrum in the absence of sound waves) is the Doppler effect. Our goal is to develop a theoretical model for a unified interpretation of the experimental data on the radial and poloidal correlation reflectometry by solving a single inverse problem. The solution of such a problem can be achieved only in the case of an analytical model of the dependence of the cross-correlation function on two variables: the spatial coordinate (minor radius of the axisymmetric toroidal plasma or the poloidal coordinate within the magnetic flux surface) and the frequency of the electric field of the scattered EM wave. The construction of an analytical model requires the identification of the main physical effects, including the Doppler effect, in the fine structure of the Mandelstam–Brillouin scattering spectrum. Currently, there are no analytical models in the literature for the cross-correlation function mentioned above.

The content of the article is as follows. Section 2 presents the basic equations for the scattering of EM waves and cross-correlation reflectometry in plasma. Section 3 proposes a physical model and the corresponding system of equations for density fluctuations, which reduces to an integral equation for the cross-correlation function of plasma density fluctuations. This equation is expressed in terms of the Holstein functional [16], which is characteristic of a wide range of nonlocal transfer processes, including the transfer of resonant radiation in plasma and gases in the Biberman–Holstein model [15–17]. In Section 4, the scattering spectrum of EM waves in a turbulent medium in a localized region of space is calculated; in Section 5, the main cross-correlation characteristics of EM wave scattering by various points of the medium are found. Section 6 formulates and solves in a particular case the inverse problem of recovering nonlocal turbulence parameters. The effectiveness of the developed approach is shown by the example of the interpretation of the data of correlation reflectometry of EM waves of the radio frequency range for diagnosing turbulent plasma in the T-10, TEXTOR, and ASDEX tokamaks.

2. Basic Equations for EM Wave Scattering and Cross-Correlation Reflectometry in Plasma

In the case of scattering of a plane monochromatic electromagnetic wave, the electric field vector of the incident wave has the form

$$\boldsymbol{E} = \boldsymbol{E}_0 e^{i\omega_i t - i\boldsymbol{k}_i \boldsymbol{\rho}}, \tag{1}$$

where ω_i is the frequency of the incident plane wave (i stands for "incident") and $\boldsymbol{k}_i$ is its wave vector. The electric field formed by the scattering of an incident wave by an ensemble of free electrons is described by the following expression (see, for example, (8.12) in [47]):

$$\boldsymbol{E}(\boldsymbol{r}, t) = \frac{r_0}{R} \int d^3\rho g(\boldsymbol{\rho}, t) e^{i(\omega_i t' - \boldsymbol{k}_i \boldsymbol{\rho})} [\hat{\boldsymbol{n}}, [\hat{\boldsymbol{n}}, \boldsymbol{E}_0]]. \tag{2}$$

Here, r_0 is the classical radius of the electron, R is the distance from the charge to the point of observation at a large distance from the electron, $g(\boldsymbol{\rho}, t)$ is the distribution function of electrons along the spatial coordinate $\boldsymbol{\rho}$ at time t, $\hat{\boldsymbol{n}}$ is the unit vector in the direction of propagation of the scattered wave, $\boldsymbol{E}_0$ is the amplitude of the electric field of the incident wave, and $t' = t - \frac{r}{c} + \frac{\hat{\boldsymbol{n}}\boldsymbol{\rho}}{c}$ (c is the speed of light). Let us denote the wave vector of the scattered wave with frequency ω_s (s means "scattered") as $\boldsymbol{k}_s = \hat{\boldsymbol{n}}\omega_s/c$, introduce the scattering vector and the scattering frequency:

$$\begin{aligned} \boldsymbol{K} &= \boldsymbol{k}_s - \boldsymbol{k}_i, \\ \omega &= \omega_s - \omega_i. \end{aligned} \tag{3}$$

Let the electrons move according to the law $\boldsymbol{\rho} = \boldsymbol{\rho}_{0,j} + \boldsymbol{v}_j t$, which corresponds to the motion of an individual particle, marked with the index j, along a straight trajectory with the initial coordinate $\boldsymbol{\rho}_{0,j}$ and velocity $\boldsymbol{v}_j$. Then the microscopic distribution function, which takes into account density fluctuations in the system of point particles, has the form:

$$g(\boldsymbol{\rho}, t) = \sum_j \delta(\boldsymbol{\rho} - \boldsymbol{\rho}_{0,j} - \boldsymbol{v}_j t), \tag{4}$$

where summation over j means summation over the contributions of individual particles. Then the electric field of the scattered radiation equation, i.e., Equation (2), takes the form

$$\begin{aligned} \boldsymbol{E}(\boldsymbol{r},t) &= \exp(i\omega_i t)[\hat{\boldsymbol{n}},[\hat{\boldsymbol{n}},\boldsymbol{E}_0]]\tfrac{r_0}{R}\int d^3\rho \sum_j \delta\left(\boldsymbol{\rho}-\boldsymbol{\rho}_{0,j}-\boldsymbol{v}_j t\right)\exp(i\boldsymbol{K}\boldsymbol{\rho}) \\ &= \exp(i\omega_i t)[\hat{\boldsymbol{n}},[\hat{\boldsymbol{n}},\boldsymbol{E}_0]]\tfrac{r_0}{R}\sum_j \exp\left[i\boldsymbol{K}\left(\boldsymbol{\rho}_{0,j}+\boldsymbol{v}_j t\right)\right], \end{aligned} \tag{5}$$

To obtain the spectral distribution of fluctuations in the density of the scattering medium, it is necessary to calculate the spectral distribution of the scattered field. In practice, the Fourier transform of the measured time dependence of the scattered field is carried out over a limited time interval, during which a statistically reliable Fourier transform can be formed. Reflectometry is characterized by time-selective probing. Therefore, it is necessary to single out the fast time t_{fast}, according to which the Fourier transform is carried out, and the slow time t_{slow}, which is a mark of various measurement time intervals, during which the macroscopic parameters of the probed medium can be considered quasi-stationary, i.e.,

$$t = t_{fast} + t_{slow}. \tag{6}$$

Then,

$$\boldsymbol{E}\left(\boldsymbol{r},t_{fast}+t_{slow}\right) = \exp\left(i\omega_i\left(t_{fast}+t_{slow}\right)\right)[\hat{\boldsymbol{n}},[\hat{\boldsymbol{n}},\boldsymbol{E}_0]]\frac{r_0}{R}\sum_j \exp\left[i\boldsymbol{K}\left(\boldsymbol{\rho}_{0,j}+\boldsymbol{v}_j\left(t_{fast}+t_{slow}\right)\right)\right]. \tag{7}$$

Let us perform the Fourier transform over fast time:

$$\hat{\boldsymbol{E}}(\boldsymbol{r},\omega_s,t_{slow}) = \frac{1}{(2\pi)^{1/2}}\int dt_{fast}\, e^{-i\omega_s t_{fast}}\boldsymbol{E}\left(\boldsymbol{r},t_{fast}+t_{slow}\right). \tag{8}$$

Taking into account Equation (7), we obtain

$$\begin{aligned} \hat{\boldsymbol{E}}(\boldsymbol{r},\omega_s,t_{slow}) = \;& \tfrac{1}{(2\pi)^{1/2}}\int dt_{fast}\, e^{-i\omega_s t_{fast}}\exp\left[i\omega_i\left(t_{fast}\right.\right. \\ & \left.\left.+t_{slow}\right)\right][\hat{\boldsymbol{n}},[\hat{\boldsymbol{n}},\boldsymbol{E}_0]]\tfrac{r_0}{R} \\ & \times\sum_j \exp\left[i\boldsymbol{K}\left(\boldsymbol{\rho}_{0,j}+\boldsymbol{v}_j\left(t_{fast}+t_{slow}\right)\right)\right] \\ & = [\hat{\boldsymbol{n}},[\hat{\boldsymbol{n}},\boldsymbol{E}_0]]\tfrac{r_0}{R}\exp[i\omega_i t_{slow}]\sum_j \exp\left[i\boldsymbol{K}\left(\boldsymbol{\rho}_{0,j}\right.\right. \\ & \left.\left.+\boldsymbol{v}_j t_{slow}\right)\right]\tfrac{1}{(2\pi)^{1/2}}\int dt_{fast}\exp\left[\left(-i\omega+i\boldsymbol{K}\boldsymbol{v}_j\right)t_{fast}\right]. \end{aligned} \tag{9}$$

We consider that the time interval of the Fourier analysis is sufficiently large, so that the well-known relation containing the Dirac delta function is satisfied with high accuracy:

$$\frac{1}{2\pi}\int dt_{fast}\exp\left[\left(-i\omega+i\boldsymbol{K}\boldsymbol{v}_j\right)t_{fast}\right] = \delta\left(\omega-\boldsymbol{K}\boldsymbol{v}_j\right). \tag{10}$$

Then,

$$\hat{\boldsymbol{E}}(\boldsymbol{r},\omega,t_{slow}) = \sqrt{2\pi}[\hat{\boldsymbol{n}},[\hat{\boldsymbol{n}},\boldsymbol{E}_0]]\frac{r_0}{R}\exp[i\omega_i t_{slow}]\sum_j \exp\left[i\boldsymbol{K}\left(\boldsymbol{\rho}_{0,j}+\boldsymbol{v}_j t_{slow}\right)\right]\delta\left(\omega-\boldsymbol{K}\boldsymbol{v}_j\right). \tag{11}$$

Let us average over the initial coordinates of the electrons. We consider separately the sum

$$\int\frac{d^3\boldsymbol{\rho}_0}{V}\sum_j \exp\left[i\boldsymbol{K}\left(\boldsymbol{\rho}_0+\boldsymbol{v}_j t_{slow}\right)\right]\delta\left(\omega-\boldsymbol{K}\boldsymbol{v}_j\right) = \int\frac{d^3\boldsymbol{\rho}_0}{V}\exp[i\boldsymbol{K}\boldsymbol{\rho}_0]\sum_j \exp\left[i\boldsymbol{K}\boldsymbol{v}_j t_{slow}\right]\delta\left(\omega-\boldsymbol{K}\boldsymbol{v}_j\right). \tag{12}$$

Note that the averaging is carried out over the volume near the observation point $\boldsymbol{r}$, for example, with radius a, so $\boldsymbol{\rho}_0 \rightarrow \boldsymbol{r} + \boldsymbol{\rho}_0'$ and

$$\int \frac{d^3\boldsymbol{\rho}_0}{V} \exp[i\boldsymbol{K}\boldsymbol{\rho}_0] = \frac{4\pi \exp[i\boldsymbol{K}\boldsymbol{r}]}{K^3 V}(\sin(Ka) - Ka\cos(Ka)). \tag{13}$$

At $a \ll 1/K$, we have $\frac{\sin(Ka) - Ka\cos(Ka)}{K^3} \approx \frac{a^3}{3}$; then assuming that $V = \frac{4}{3}\pi a^3$, we finally have

$$\int \frac{d^3\boldsymbol{\rho}_0}{V} \exp[i\boldsymbol{K}\boldsymbol{\rho}_0] \approx \exp[i\boldsymbol{K}\boldsymbol{r}]. \tag{14}$$

Then,

$$\begin{aligned} \hat{\boldsymbol{E}}(\boldsymbol{r}, \omega, t_{slow}) &= \sqrt{2\pi}[\hat{\boldsymbol{n}}, [\hat{\boldsymbol{n}}, \boldsymbol{E}_0]] \tfrac{r_0}{R} \exp[i\omega_i t_{slow} - i\boldsymbol{K}\boldsymbol{r}] \sum_j \exp\left[i\boldsymbol{K}\boldsymbol{v}_j t_{slow}\right] \delta\left(\omega - \boldsymbol{K}\boldsymbol{v}_j\right) \\ &= \sqrt{2\pi}[\hat{\boldsymbol{n}}, [\hat{\boldsymbol{n}}, \boldsymbol{E}_0]] \tfrac{r_0}{R} \exp[i\omega_s t_{slow} - i\boldsymbol{K}\boldsymbol{r}] \sum_j \delta\left(\omega - \boldsymbol{K}\boldsymbol{v}_j\right). \end{aligned} \tag{15}$$

It can be seen that the result for the spectrum of scattered radiation field described by Equation (15) includes the sum of the Fourier transforms of the density of individual electrons; therefore, taking into account Equation (4), we can write

$$\breve{g}(\omega,\ \boldsymbol{K}) = \sum_j \delta\left(\omega - \boldsymbol{K}\boldsymbol{v}_j\right). \tag{16}$$

Then Equation (15) can be rewritten in the following form, omitting the dependence on the slow variable t_{slow} and renaming $R = |\boldsymbol{r}|$:

$$\hat{\boldsymbol{E}}(\boldsymbol{r}, \omega, \boldsymbol{K}) = \sqrt{2\pi}[\hat{\boldsymbol{n}}, [\hat{\boldsymbol{n}}, \boldsymbol{E}_0]] e^{-i(\boldsymbol{K}, \boldsymbol{r})} \frac{r_0}{|\boldsymbol{r}|} \breve{g}(\omega,\ \boldsymbol{K}). \tag{17}$$

The spectral-angular distribution of the radiation power scattered by a charged particle with a classical radius r_0 from point r to point r_1 at time t (we neglect the delay of scattered diagnostic EM waves) has the form (see, for example, (8.15) and (8.18) in [47]):

$$\frac{dW(\omega, \hat{\boldsymbol{n}}, \boldsymbol{r}_1, t)}{d\Omega_{\hat{\boldsymbol{n}}}\, d\omega_s} = \frac{c{r_0}^2}{4\pi} [\hat{\boldsymbol{n}}, [\hat{\boldsymbol{n}}, \boldsymbol{E}_0]]^2 \lim_{T_0 \to \infty} \frac{1}{\pi T_0} |\breve{g}(\omega,\ \boldsymbol{K}, \boldsymbol{r}, t, T_0)|^2, \tag{18}$$

where the Fourier transform means the corresponding transformation in fast variables (i.e., over a limited interval, practically sufficient for reliable calculation of the Fourier transform); $\hat{\boldsymbol{n}}$ is the unit vector in the direction of propagation from point $\boldsymbol{r}$ to point $\boldsymbol{r}_1$; and $\Omega_{\hat{\boldsymbol{n}}}$ is the corresponding solid angle. Adding the coordinate $\boldsymbol{r}$ to the function argument means binding all parameters to a "slow" spatial variable, and the time integrals in calculating the Fourier transform of the density should be taken on a limited time interval $[0, T_0]$ near the (slow) time t. The time averaging operation T_0 is necessary to find the spectral composition of the power (and not the entire energy) of the scattered radiation.

We will use the standard definition of the cross-correlation function of the scattered field, $C(\widetilde{\tau})$, as a convolution (in fast time) of scattering signals from two points $\boldsymbol{r}_1$ and $\boldsymbol{r}_2$ in the coordinate space:

$$C(\widetilde{\tau}, \boldsymbol{r}_1, \boldsymbol{r}_2) = \frac{\int_{-\infty}^{+\infty} dt \boldsymbol{E}^*(\boldsymbol{r}_1, t, \boldsymbol{K}_1) \boldsymbol{E}(\boldsymbol{r}_2, t + \widetilde{\tau}, \boldsymbol{K}_2)}{\left[\int_{-\infty}^{+\infty} dt |\boldsymbol{E}(\boldsymbol{r}_1, t, \boldsymbol{K}_1)|^2 \int_{-\infty}^{+\infty} dt |\boldsymbol{E}(\boldsymbol{r}_2, t, \boldsymbol{K}_2)|^2\right]^{1/2}}. \tag{19}$$

The electric fields in Equation (19) are determined by Equation (17), which includes statistical averaging over the electron parameters, which assumes the sum over j in Equation (16).

The Fourier transform of the function in Equation (19) with respect to the delay time $\widetilde{\tau}$ gives the spectral distribution, which is the final result of processing the experimental data of cross-correlation reflectometry:

$$C(\omega, \boldsymbol{r}_1, \boldsymbol{r}_2) = \frac{\lim\limits_{T_0 \to \infty} \frac{1}{T_0} \hat{\boldsymbol{E}}^*(\boldsymbol{r}_1, \omega, \boldsymbol{K}_1) \hat{\boldsymbol{E}}(\boldsymbol{r}_2, \omega, \boldsymbol{K}_2)}{\sqrt{\lim\limits_{T_{01} \to \infty} \left(\frac{1}{T_{01}} \left| \hat{\boldsymbol{E}}(\boldsymbol{r}_1, \omega, \boldsymbol{K}_1) \right|^2 \right) \lim\limits_{T_{02} \to \infty} \left(\frac{1}{T_{02}} \left| \hat{\boldsymbol{E}}(\boldsymbol{r}_2, \omega, \boldsymbol{K}_2) \right|^2 \right)}} \tag{20}$$

where $\hat{\boldsymbol{E}}(\boldsymbol{r}_1, \omega, \boldsymbol{K}_1)$ is the Fourier transform in time of the electric field of the scattered EM wave. In this case, in Equation (20), statistical averaging over the parameters of scatterers is assumed, which corresponds to averaging over all microscopic parameters of electrons in the distribution function in Equation (4).

3. Kinetic Model of Density Fluctuations in a Turbulent Medium

To describe the nonlocality of the transfer of density perturbations in a turbulent medium, we will use the hypothesis [34] on the possibility of representing the dynamics of localized perturbations of the medium using a linear integral–differential equation with an integral over spatial variables. The kernel of such an integral is a slowly decreasing function of coordinates, and the corresponding probability of a free path of carriers of a disturbance in the medium belongs to the class of Lévy distributions. This approach assumes that strong nonlinear interactions form an ensemble of stable long-lived perturbations of the medium (for example, wave packets with the properties of solitons) that interact with the medium (are produced and absorbed in it) in a balance mode described by linear kinetic equations. Although the formalism proposed by us differs significantly from the formalism of [34], in the conceptual aspect, we actually follow the hypothesis of [34].

We propose such an implementation of the approach [34] in which the stochastic properties of a medium with a strong nonlocality of the transfer of perturbations of its density are described by a formalism such as nonlocal transfer of photons in the medium in the Biberman–Holstein model [15,16]. This model is widely known as the transfer of resonant radiation in the approximation of complete redistribution (CRD) of the frequency of a photon in the elementary act of absorption of a photon by atoms or ions and its subsequent emission by an excited atom or ion (for more details, see, for example, monographs [17,23] and reviews [20,21,27]). Note that the property of forgetting the spectral-angular parameters of a photon when it is re-emitted by an excited atom within the same spectral line is quite acceptable when using this approach to describe stochastic processes in a turbulent medium. To describe the transfer processes of density perturbations in the problems of reflectometry that are of interest to us, it is necessary to move from the limiting case of infinite velocity of carriers, applicable to the motion of photons in laboratory plasma and used in the standard Biberman–Holstein model, to the case of the finite velocity of the carriers. In terms of nonlocal (i.e., superdiffusion) transport properties, this means a transition from Lévy flights [1–5] to Lévy walks [6–9]. Accounting for the finite speed of light is typical for problems of radiation transfer in astrophysical objects [10–13], but the problems of nonstationary nonlocal transfer were considered only for the infinite speed of light, and the finiteness of the speed of light was taken into account in the problems of transfer of monochromatic radiation, which is not a superdiffusion. Problems of nonstationary nonlocal transport for a finite fixed velocity of carriers were recently solved, in [29–33], including the tracing in [31] of the transition between transport modes dominated by flights or Lévy walks, i.e., between modes, when, respectively, it is appropriate or inappropriate to neglect the effects of delay due to the finiteness of the velocity of the carriers.

The application of the concept of Lévy walks to the transport of density perturbations in a quasi-homogeneous quasi-stationary medium means that the proposed model assumes the following microscopic dynamics. Localized density perturbations generated as a result of strong nonlinear processes can either remain trapped by the medium, almost not moving relative to the medium (we will call them standing excitations of the medium), or (as localized nonlinear waves of the soliton type) move at a constant speed until the act of "absorption" by the medium of a moving (traveling) excitation. By absorption, we mean the capture (stopping) of a traveling excitation, i.e., its transformation into a standing excitation of the medium with a finite lifetime, after which the standing excitation of the medium turns into a traveling excitation. The process of birth of standing excitations is an elementary mechanical process in the sense that there is also an inverse process of destruction (quenching) when the energy of a localized perturbation of the medium is returned to the medium as a whole, i.e., delocalized by certain inelastic processes. The law of motion of traveling excitations is determined by the dispersion properties of nonlinear waves in the medium and assumes the presence of some velocity distribution. Plasma density fluctuations, which are of interest to us in the problem of reflectometry, can be considered as localized perturbations of a quasi-homogeneous quasi-stationary medium and the formalism of the Biberman–Holstein model can be applied to them, taking into account the finite velocity of the perturbation carriers. At the same time, we will characterize the stochastic properties of the processes of birth and annihilation (extinguishing), free path in the medium, and stopping ("absorption" of a traveling fluctuation) of the elementary excitation of the medium by phenomenologically introduced spectral probabilities. The main parameters of these probability distributions are to be restored by solving the inverse problem when interpreting the results of measurements of the scattering spectra of diagnostic radiation and its cross-correlation reflectometry.

Let us consider the system of nonlocal transport equations for the intensity $I_{\widetilde{\omega}}(\boldsymbol{r},\boldsymbol{n},t)$ (i.e., the energy flux density) of traveling fluctuations (carriers) and the density of standing fluctuations $f(\boldsymbol{\rho},t)$ in dimensional variables for one kind of carriers:

$$\begin{aligned} &\tfrac{\partial f(\boldsymbol{r},t)}{\partial t} = -\Big(\tfrac{1}{\tau}+\sigma\Big) f(\boldsymbol{r},t) + \int d\widetilde{\omega}\, \tfrac{\kappa_{\widetilde{\omega}}}{\hbar\widetilde{\omega}} \int d\Omega(\boldsymbol{n}) I_{\widetilde{\omega}}(\boldsymbol{r},\boldsymbol{v},t) + q(\boldsymbol{r},t), \\ &\tfrac{1}{v}\tfrac{\partial I_{\widetilde{\omega}}(\boldsymbol{r},\boldsymbol{v},t)}{\partial t} + (\boldsymbol{n},\nabla) I_{\widetilde{\omega}}(\boldsymbol{r},\boldsymbol{v},t) = -\kappa_{\widetilde{\omega}} I_{\widetilde{\omega}}(\boldsymbol{r},\boldsymbol{v},t) + \tfrac{\hbar\widetilde{\omega}}{\tau}\tfrac{P_{\widetilde{\omega}}}{4\pi} f(\boldsymbol{r},t). \end{aligned} \tag{21}$$

Here, τ is the average lifetime of standing fluctuations; σ is the average inverse time for the disappearance of standing fluctuations ("quenching" of the excitation of the medium); $\boldsymbol{v}$ is the speed of movement of traveling density fluctuations, which are elementary "scatterers" of diagnostic waves, just as, for example, charged particles are "scatterers" of EM waves (in the case of noncollective scattering, this is called Thomson scattering for weakly relativistic particles and Compton scattering for relativistic particles), $\boldsymbol{v} = \boldsymbol{n}v$; $P_{\widetilde{\omega}}$ is the spectral distribution of the probability of emission of carriers with frequency $\widetilde{\omega}$; $\kappa_{\widetilde{\omega}}$ is the coefficient of "absorption" of carriers with frequency $\widetilde{\omega}$ (i.e., the reciprocal free path of such carriers before stopping in the medium); and $q(\boldsymbol{r},t)$ is the source of standing fluctuations (the power density of the production of such fluctuations in the medium).

When describing nonlocal (superdiffusion) transport, it is convenient to use the following functionals (in the three-dimensional case) (cf, for example, Section 1 in [20]):

$$W(\rho) = -\frac{1}{4\pi\rho^2}\frac{dT(\rho)}{d\rho} \equiv \frac{1}{4\pi\rho^2} W_{step}(\rho), \qquad T(\rho) = \int d\widetilde{\omega}\; P_{\widetilde{\omega}} \exp[-\kappa_{\widetilde{\omega}}\rho], \tag{22}$$

In this case, the function $W_{step}(\rho)$ is the free path distribution function, the so-called step-length probability density function (PDF) of carriers of disturbances in the medium. The integral in Equation (22) is taken over all frequencies. Note also that the spectral characteristics of the source and sink for traveling density fluctuations depend on the velocity of these fluctuations. In what follows, we will explicitly indicate this dependence.

It is important to note that the frequency $\widetilde{\omega}$ used here is such a characteristic of perturbation carriers that allows one to describe the dispersion of their free paths. The frequency in Equations (21) and (22) can be interpreted as a fluctuating energy of carriers (in the Biberman–Holstein model, the frequency of resonant radiation is uniquely related to the energies of the corresponding elementary perturbations of the electrodynamic vacuumphotons) and significantly affects the mean free path. In what follows, we reduce the description of the final results in terms of the Holstein function and thus construct a formalism in which the dependence on the details of the spectral characteristics of the elementary acts of emission and absorption of carriers is concentrated in the dependence of the Holstein function on the spatial coordinate, which describes the probability of the free path no less than a given distance.

To implement superdiffusion transport, the step-length PDF must be a slowly decreasing function of the distance ρ, i.e., a power function (in dimensional form):

$$W_{step}(\rho, \boldsymbol{v}) = \frac{\gamma\kappa_0(\boldsymbol{v})}{(1+\kappa_0(\boldsymbol{v})\rho)^{\gamma+1}}, \quad T(\rho, \boldsymbol{v}) = \frac{1}{(1+\kappa_0(\boldsymbol{v})\rho)^{\gamma}}, 0 < \gamma < 2, \tag{23}$$

where $1/\kappa_0(\boldsymbol{v})$ is the characteristic free path of carriers (traveling fluctuations) moving with a (constant) velocity $\boldsymbol{v}$.

For the problem of scattering of diagnostic EM waves, we will be interested in the Fourier transform of the fluctuation density in space and time variables, since the electric field of the scattered EM wave is determined by the Fourier transform of the fluctuation density at a frequency value equal to $\omega = \omega_s - \omega_i$, and the wave vector, equal to $\boldsymbol{K} = \boldsymbol{k}_s - \boldsymbol{k}_i$ (where the index s means the scattered wave and i the incident). Thus, the frequency ω indicated here has a different meaning than that in Equations (21) and (22).

In the system of Equation (21), we will assume that the dynamics of carriers occur in a weakly inhomogeneous quasi-stationary medium, which is further understood as a medium with characteristic spatio-temporal scales of change in the parameters σ, $\kappa_{\widetilde{\omega}}$, and $P_{\widetilde{\omega}}$, which are much larger than the corresponding parameters of the carrier distribution function. Then, when solving the system of kinetic equations using the Fourier and Laplace transformations with respect to "fast" variables, the specified parameters of the medium can be considered constant ("slow" variables).

After Fourier transformations with respect to the spatial coordinate, the system in Equation (21) takes the form

$$\begin{aligned} &\frac{\partial \hat{f}(\boldsymbol{K},t)}{\partial t} = -\left(\frac{1}{\tau}+\sigma\right)\hat{f}(\boldsymbol{K},t) + \int d\widetilde{\omega}\frac{\kappa_{\widetilde{\omega}}}{\hbar\widetilde{\omega}}\int d\Omega(\boldsymbol{n})\hat{I_{\widetilde{\omega}}}(\boldsymbol{K},\boldsymbol{n},t) + \hat{q}(\boldsymbol{K},t) = 0 \\ &\frac{1}{v}\frac{\partial \hat{I_{\widetilde{\omega}}}(\boldsymbol{K},\boldsymbol{v},t)}{\partial t} - i(\boldsymbol{n},\boldsymbol{K})\hat{I_{\widetilde{\omega}}}(\boldsymbol{K},\boldsymbol{v},t) = -\kappa_{\widetilde{\omega}}\hat{I_{\widetilde{\omega}}}(\boldsymbol{K},\boldsymbol{v},t) + \frac{\hbar\widetilde{\omega}}{\tau}\frac{1}{4\pi}P_{\widetilde{\omega}}\hat{f}(\boldsymbol{K},t) \end{aligned} \tag{24}$$

The solution of the second equation in the system with the initial condition $\hat{I_{\widetilde{\omega}}}(\boldsymbol{K},\boldsymbol{v},0) = 0$ has the following form for $t > 0$:

$$\hat{I_{\widetilde{\omega}}}(\boldsymbol{K},\boldsymbol{v},t) = \frac{\hbar\widetilde{\omega}}{\tau}\frac{v}{4\pi}P_{\widetilde{\omega}}\int_0^t dt' \exp\left[-v(t-t')\{-i(\boldsymbol{n},\boldsymbol{K})+\kappa_{\widetilde{\omega}}\}\right]\hat{f}(\boldsymbol{K},t'). \tag{25}$$

Then the first part in Equation (24) can be rewritten as:

$$\frac{\partial \hat{f}(\boldsymbol{K},t)}{\partial t} = -\left(\frac{1}{\tau}+\sigma\right)\hat{f}(\boldsymbol{K},t) + \frac{1}{\tau}\int_0^t dt' \hat{f}(K,t')y(\boldsymbol{K},t-t',v) + \hat{q}(\boldsymbol{K},t), \tag{26}$$

where, taking into account Equations (22) and (23), the function y is as follows:

$$y(K,t,v) = \frac{4\pi}{K}v^2 tW(vt)\sin(vtK) = \frac{\gamma\kappa_0}{(1+vt\kappa_0)^{\gamma+1}}\frac{\sin(vtK)}{tK}. \tag{27}$$

We will solve Equation (26) using the Laplace transform with respect to the fast time variable, assuming $\hat{f}(\boldsymbol{K},0) = 0$:

$$\hat{f}(\boldsymbol{K},t) \Rightarrow F(\boldsymbol{K},s), \quad y(\boldsymbol{K},t,v) \Rightarrow Y(\boldsymbol{K},s,v). \tag{28}$$

Then we have

$$F(\boldsymbol{K},s) = \frac{Q(\boldsymbol{K},s)}{s + 1/\tau + \sigma - 1/\tau Y(K,s,v)}, \tag{29}$$

where

$$Y(K,s) = \int_{0}^{+\infty} e^{-st'} y(K,t')dt' = \frac{\gamma\kappa_0}{K} \int_{0}^{+\infty} \frac{dt'\, e^{-st'}}{(1+vt'\kappa_0)^{\gamma+1}} \frac{\sin(vKt')}{t'}. \tag{30}$$

As a result, for the transform function, we obtain the expression

$$\hat{f}(\boldsymbol{K},t) = \frac{1}{2\pi i} \int_{+0-i\infty}^{+0+i\infty} e^{st} F(\boldsymbol{K},s)ds = \frac{1}{2\pi i} \int_{+0-i\infty}^{+0+i\infty} \frac{ds\, e^{st} Q(\boldsymbol{K},s)}{s + 1/\tau + \sigma - 1/\tau Y(K,s,v)}. \tag{31}$$

Let us turn to the result of Equation (25), i.e., the equation for intensity, with Equation (31) taken into account. Then

$$\hat{I_{\widetilde{\omega}}}(\boldsymbol{K},\boldsymbol{v},t) = \frac{\hbar\widetilde{\omega}}{\tau} \frac{v}{4\pi} \frac{P_{\widetilde{\omega}}}{2\pi i} \int_{+0-i\infty}^{+0+i\infty} \frac{ds\, Q(\boldsymbol{K},s)}{s + 1/\tau + \sigma - 1/\tau Y(K,s,v)} \times \int_{0}^{t} dt' \exp\left[-v(t-t')\{-i(\boldsymbol{n},\boldsymbol{K}) + \kappa_{\widetilde{\omega}}\} + st'\right]. \tag{32}$$

The inner integral here can be calculated for $t > 0$,

$$\int_{0}^{t} dt_2 \exp[-v(t-t_2)\{-i(\boldsymbol{n},\boldsymbol{K}) + \kappa_{\widetilde{\omega}}\} + st_2] = \frac{e^{st} - e^{-vt\{-i(\boldsymbol{nK})+\kappa_{\widetilde{\omega}}\}}}{v\{-i(\boldsymbol{n},\boldsymbol{K}) + \kappa_{\widetilde{\omega}}\} + s}\theta(t). \tag{33}$$

Then

$$\hat{I_{\widetilde{\omega}}}(\boldsymbol{K},\boldsymbol{n},t,v) = \frac{\hbar\widetilde{\omega}}{\tau} \frac{v}{4\pi} \frac{P_{\widetilde{\omega}}}{2\pi i}\theta(t) \int_{+0-i\infty}^{+0+i\infty} \frac{ds\, Q(\boldsymbol{K},s)}{s + 1/\tau + \sigma - 1/\tau Y(K,s,v)} \frac{e^{st} - e^{-vt\{-i(\boldsymbol{n},\boldsymbol{K})+\kappa_{\widetilde{\omega}}\}}}{v\{-i(\boldsymbol{n},\boldsymbol{K}) + \kappa_{\widetilde{\omega}}\} + s}. \tag{34}$$

Let us define the density of fluctuations traveling with a speed $\boldsymbol{v}$, which is an integral value over the energy of individual carriers (the frequency $\widetilde{\omega}$ in Equation (21)), and we will look for the Fourier transform of this function with respect to the spatial coordinate:

$$\hat{g}(\boldsymbol{K},t,v) = \frac{1}{v} \int d\widetilde{\omega} \frac{\hat{I_{\widetilde{\omega}}}(\boldsymbol{K},v,t)}{\hbar\widetilde{\omega}}, \tag{35}$$

where $\hat{I_{\widetilde{\omega}}}(\boldsymbol{K},v,t)$ is the Fourier transform of the intensity with respect to the spatial coordinate. Then, taking into account Equation (34), we have the following expression for $\hat{g}$:

$$\hat{g}(\boldsymbol{K},t,\boldsymbol{v}) = \frac{1}{4\pi} \frac{\theta(t)}{2\pi i} \int d\widetilde{\omega} P_{\widetilde{\omega}} \int_{+0-i\infty}^{+0+i\infty} \frac{ds\, Q(\boldsymbol{K},s)}{s\tau + 1 + \sigma\tau - Y(K,s,v)} \frac{e^{st} - e^{-vt\{-i(\boldsymbol{n},\boldsymbol{K})+\kappa_{\widetilde{\omega}}\}}}{v\{-i(\boldsymbol{n},\boldsymbol{K}) + \kappa_{\widetilde{\omega}}\} + s}\theta(t). \tag{36}$$

A factor

$$Q(\boldsymbol{K},s)/(s\tau + 1 + \sigma\tau - Y(K,s,v))$$

in Equation (36) describes the renormalization of the source of standing fluctuations. The term $\sigma\tau$ corresponds to the number of "quenchings" of standing excitations of the medium during their lifetime. The function Y describes the contribution of the medium excitation transfer process: as the path length of traveling fluctuations in this factor in Equation (36) tends to zero (i.e., the "absorption" coefficient tends to infinity), only the term $\sigma\tau$ remains in the denominator, which corresponds to the limit of thermodynamic equilibrium with respect to the birth and annihilation of standing excitations of the medium. In this case, the relationship between the source and the sink of the excitation of the medium (in this case, the standing excitation of the medium is the standing density fluctuations) is expressed in terms of the flux density of the carriers of the excitation of the medium (in this case, the carriers of the excitation of the medium are traveling fluctuations) and is an analog of the Kirchhoff law for radiation.

For the spectrum of the density of traveling fluctuations $\hat{g}$ from Equation (36), by means of the Laplace transform, we obtain the following expression:

$$\begin{aligned}\breve{g}(\boldsymbol{K},\omega,\boldsymbol{v}) = {} & \tfrac{1}{(2\pi)^2}\tfrac{1}{2\tau}\sqrt{\tfrac{\pi}{2}}\tfrac{Q(\boldsymbol{K},i\omega)}{+i\omega+1/\tau+\sigma-1/\tau Y(K,i\omega,v)}\int d\widetilde{\omega}P_{\widetilde{\omega}}\tfrac{1}{v\{-i(\boldsymbol{n},\boldsymbol{K})+\kappa_{\widetilde{\omega}}\}+i\omega} \\ & +\tfrac{1}{(2\pi)^{5/2}}\tfrac{1}{2\tau i}\int d\widetilde{\omega}P_{\widetilde{\omega}}\int\limits_{+0-i\infty}^{+0+i\infty}\tfrac{ds\ Q(\boldsymbol{K},s)}{s+1/\tau+\sigma-1/\tau Y(K,s,v)} \\ & \times\tfrac{1}{v\{-i(\boldsymbol{n},\boldsymbol{K})+\kappa_{\widetilde{\omega}}\}+s}\left(-\tfrac{1}{s-i\omega}-\tfrac{1}{v\{-i(\boldsymbol{n},\boldsymbol{K})+\kappa_{\widetilde{\omega}}\}+i\omega}\right).\end{aligned} \tag{37}$$

Integration of the second term $\sim \frac{1}{v\left\{-i(\boldsymbol{n},\boldsymbol{K})+\kappa_{\widetilde{\omega}_1}\right\}+i\omega}$ in parentheses gives zero, because when closing through the right half-plane, it has no poles (closing through the right half-plane is necessary for the convergence of $Y(K,s,v)$).

Let us consider in more detail the pole at point $s=+i\omega$. Since at $\alpha\to 0$, the singular point is on the integration axis, it is necessary to bypass this pole along an infinitely small semicircle on the left according to the bypass rule. Therefore, the contribution to the integral from a given pole is determined by the semiresidue of the integrand. Then, for the density spectrum of traveling density fluctuations, we have the expression:

$$\begin{aligned}\breve{g}(\boldsymbol{K},\omega,\boldsymbol{v}) = {} & \tfrac{1}{(2\pi)^{3/2}}\tfrac{1}{2\tau}\tfrac{Q(\boldsymbol{K},i\omega)}{i\omega+1/\tau+\sigma-1/\tau Y(K,i\omega,v)}\int d\widetilde{\omega}P_{\widetilde{\omega}}\tfrac{1}{v\{-i(\boldsymbol{n},\boldsymbol{K})+\kappa_{\widetilde{\omega}}\}+i\omega} \\ & -\tfrac{i}{(2\pi)^{5/2}}\tfrac{1}{2\tau}\int\limits_{-\infty}^{+\infty}\tfrac{dy\ Q(\boldsymbol{K},iy)}{iy+1/\tau+\sigma-1/\tau Y(K,iy,v)}P\tfrac{1}{y-\omega}\int d\widetilde{\omega}P_{\widetilde{\omega}}\tfrac{1}{v\{-i(\boldsymbol{n},\boldsymbol{K})+\kappa_{\widetilde{\omega}}\}+iy}.\end{aligned} \tag{38}$$

Let us pay attention to the integrand in the second term in Equation (38). It means the following:

$$\frac{1}{v\{-i(\boldsymbol{n},\boldsymbol{K})+\kappa_{\widetilde{\omega}}\}+i\omega}=\sqrt{2\pi}\int\limits_{-\infty}^{+\infty}dte^{-i\omega t}e^{-vt\{-i(\boldsymbol{n},\boldsymbol{K})+\kappa_{\widetilde{\omega}}\}}\theta(t).$$

Consider the integral in the first term in Equation (38), taking into account the integrand and also Equation (22). Then it can be expressed in terms of the Holstein functional $T(vt,\boldsymbol{v})$:

$$\int d\widetilde{\omega}P_{\widetilde{\omega}}\frac{1}{v\{-i(\boldsymbol{n},\boldsymbol{K})+\kappa_{\widetilde{\omega}}\}+i\omega}=\sqrt{2\pi}\int\limits_{0}^{+\infty}dte^{-i(\omega-(\boldsymbol{v},\boldsymbol{K}))t}T(vt,\boldsymbol{v})$$

Here, we have explicitly specified the second argument (velocity of the carrier) in the Holstein function (cf Equation (23)). Then, for the spectrum, we have the following expression:

$$\begin{aligned}\breve{g}(\boldsymbol{K},\omega,\boldsymbol{v}) = {} & \tfrac{1}{4\pi}\tfrac{Q(\boldsymbol{K},i\omega)}{1+\sigma\tau+i\omega\tau-Y(K,i\omega,v)}\int\limits_{0}^{+\infty}dte^{-i(\omega-(\boldsymbol{v},\boldsymbol{K}))t}T(vt,\boldsymbol{v}) \\ & -\tfrac{i}{2(2\pi)^2}\int\limits_{-\infty}^{+\infty}\tfrac{dy\ Q(\boldsymbol{K},iy)}{1+\sigma\tau+i\tau y-Y(K,iy,v)}P\tfrac{1}{y-\omega}\int\limits_{0}^{+\infty}dte^{-i(y-(\boldsymbol{v},\boldsymbol{K}))t}T(vt,\boldsymbol{v}).\end{aligned} \tag{39}$$

The main contribution to the density of traveling fluctuations is made by the first term, so the result for the Fourier–Laplace transform of their density is expressed in terms of the Holstein functions shown in Equations (22) and (23), which describes the measure of nonlocality (superdiffusion) of the transfer process. Taking into account the constancy of the velocity of the carrier already indicated above as it moves from the point of birth to the point of stopping, we have the following expression for the contribution of the j-th particle of the m-th kind to the Fourier–Laplace transform of the fluctuation density:

$$\breve{g}_m(\boldsymbol{K},\omega,\boldsymbol{v}_j) = \frac{1}{4\pi} Q_{eff}{}^{(m)}(\boldsymbol{K},i\omega,v_j) \int\limits_0^{+\infty} dt e^{-i(\omega-(\boldsymbol{v}_j,\boldsymbol{K}))t} T_m(v_j t,\boldsymbol{v}_j). \tag{40}$$

which is the product of the renormalized (effective) source of standing fluctuations

$$Q_{eff}{}^{(m)}(\boldsymbol{K},i\omega,v_j) = \frac{Q_m(\boldsymbol{K},i\omega)}{1+\sigma_m\tau_m + i\omega\tau_m - Y_m(K,i\omega,v_j)}, \tag{41}$$

on the Fourier transform of the Holstein function taking into account the Doppler frequency shift in the act of scattering of the probing radiation by a traveling fluctuation. Here, $Q_m(\boldsymbol{K},i\omega)$ is the Fourier–Laplace transform for the source of standing fluctuations of sort m, $q(\boldsymbol{r},t)$ in Equation (21).

Further, we will use an approximate expression for an effective source at $\sigma\tau \gg \omega\tau \gg 1$ (thermodynamic limit for the density of standing fluctuations).

As will be shown below, in practical problems, we will be interested in such a case when the effect of "absorption" of carriers (traveling fluctuations of density), caused by the finiteness of their free paths, will be small compared to the effect of the Doppler broadening of the spectra due to the motion of carriers. This means that the integral in Equation (40) is close to the Dirac delta function, since as the absorption coefficient formally tends to zero, the Holstein function tends to unity, and we have:

$$\lim_{\kappa_0\to 0} \breve{g}_m(\boldsymbol{K},\omega,\boldsymbol{v}_j) = \frac{1}{8} \frac{Q_m(\boldsymbol{K},i\omega)}{1+\sigma_m\tau_m + i\omega\tau_m} \delta(\omega - (\boldsymbol{v}_j,\boldsymbol{K})). \tag{42}$$

This limit of free motion of density fluctuations is important for checking the coincidence of the scattering spectrum with that in the well-known problem of noncollective scattering of EM radiation by free particles.

4. Scattering Spectrum

To calculate the spectrum of scattered radiation, let us turn to the scattering spectrum (Equation (18)) on particles of type m. Taking into account Equation (40), it takes the form:

$$\begin{aligned} &\frac{dW_m(\omega,\hat{\boldsymbol{n}},\boldsymbol{r}_1,t)}{d\Omega_{\hat{\boldsymbol{n}}}\, d\omega_s} \\ &= \frac{c r_0{}^2}{(4\pi)^3} \left| \sum_j Q_{eff}{}^{(m)}(\boldsymbol{K},i\omega,v_j) \int\limits_0^{T_0} dt e^{-i(\omega-(\boldsymbol{v}_j,\boldsymbol{K}))t} T_m(v_j t,\boldsymbol{v}_j) \right|^2. \end{aligned} \tag{43}$$

$$\begin{aligned} &\left| \sum_j Q_{eff}{}^{(m)}(\boldsymbol{K},i\omega,v_j) \int\limits_0^{T_0} dt e^{-i(\omega-(\boldsymbol{v}_j,\boldsymbol{K}))t} T_m(v_j t,\boldsymbol{v}_j) \right|^2 \\ &\qquad = \sum_j \left| Q_{eff}{}^{(m)}(\boldsymbol{K},i\omega,v_j) \right|^2 \left| \int\limits_0^{T_0} dt e^{-i(\omega-(\boldsymbol{v}_j,\boldsymbol{K}))t} T_m(v_j t,\boldsymbol{v}_j) \right|^2. \end{aligned} \tag{44}$$

Note that after this step, the summation in the only remaining sum over particles can be replaced by integration over the continuum distribution function of scattering particles over velocities.

The next simplification is related to the assumption of perturbativity, i.e., the smallness of the broadening of the Dirac delta function by the effect of the finite lifetime of carriers due to their absorption (in our case, stopping of traveling fluctuations). When the absorption of carriers in Equation (44) is completely neglected, the passage to the limit $T_0 \to \infty$ gives the transformation of the square of the delta function (Equation (42)) to its first power (see, for example, (8.16) in [47] and Equation (7) in [48]). Within the framework of the perturbative consideration of absorption, one of the integrals can be set to $T(0,v) = 1$, which gives the following expression for the spectrum of radiation scattered by a particle with velocity $\boldsymbol{v}$:

$$\begin{aligned} &\frac{dW_m(\omega,\hat{\boldsymbol{n}},\boldsymbol{v},\boldsymbol{r}_1,t)}{d\Omega_{\hat{n}}\ d\omega_s} \\ &= \frac{c{r_0}^2}{\pi(4\pi)^3}\left[\hat{\boldsymbol{n}},[\hat{\boldsymbol{n}},\boldsymbol{E}_0]\right]^2 \left|Q_{eff}(\boldsymbol{K},i\omega,\boldsymbol{v})\right|^2 \left|\int\limits_0^{+\infty} dt e^{-i(\omega-(\boldsymbol{v},\boldsymbol{K}))t} T_m(vt,v)\right| \end{aligned} \tag{45}$$

The result of Equation (45) (without an effective source) differs from the well-known expression for the spectrum of noncollective scattering of probing radiation by free charged particles by the presence of the Holstein function in the integrand, which corresponds to the broadening of the spectral line of the scattered radiation due to the finite lifetime of the scatterer (compare, for example, (8.35) in [47], as well as Equation (14) in [48] and a discussion there of the details of averaging over time T_0 and the corresponding accurate passage to an infinite upper limit in the integral over time).

For a particular form of the Holstein function (Equation (23)), the time integral in Equation (45) can be calculated analytically. For $\gamma \neq 1$, we obtain (in Equations (46) and (47), the index m for the sort of scattering particles is omitted):

$$\begin{aligned} &\int\limits_0^{+\infty} dt e^{-i(\omega-(\boldsymbol{v},\boldsymbol{K}))t} T(vt,v) = \int\limits_0^{+\infty} dt \frac{e^{-i(\omega-(\boldsymbol{v},\boldsymbol{K}))t}}{(1+\kappa_0 vt)^\gamma} \\ &= -\frac{1}{(1-\gamma)\kappa_0 v} F_{12}\left([1],\left[1-\tfrac{\gamma}{2},\tfrac{3}{2}-\tfrac{\gamma}{2}\right],-\left(\tfrac{p}{2}\right)^2\right) + \frac{\pi\ \sin\left(\frac{\gamma\pi}{2}+p\right)}{\Gamma(\gamma)\sin(\gamma\pi)|\omega-(\boldsymbol{v},\boldsymbol{K})|^{1-\gamma}(\kappa_0 v)^\gamma} \\ &-i\frac{1}{(\omega-(\boldsymbol{v},\boldsymbol{K}))\sin(\gamma\pi)}\left\{\frac{\pi p^\gamma}{\Gamma(\gamma)}\cos\left(\frac{\gamma\pi}{2}+p\right)\right. \\ &\left.+\frac{\sin(\gamma\pi)p^2}{(2-\gamma)(1-\gamma)} F_{12}\left([1],\left[\tfrac{3}{2}-\tfrac{\gamma}{2},2-\tfrac{\gamma}{2}\right],-\left(\tfrac{p}{2}\right)^2\right)\right\}, \end{aligned} \tag{46}$$

where F_{12} is the generalized hypergeometric function, and in the absorption coefficient κ_0, for ease of notation, its dependence on velocity v is omitted. For $\gamma = 1$, we find:

$$\begin{aligned} &\int\limits_0^{+\infty} dt e^{-i(\omega-(\boldsymbol{v},\boldsymbol{K}))t} T(vt,v) \\ &\qquad = \frac{1}{\kappa_0 v}\left\{-\cos(p)\mathrm{Ci}(p) + \sin(p)\left(\tfrac{\pi}{2}-\mathrm{Si}(p)\right)\right\} \\ &\qquad -i\frac{\mathrm{sign}(\omega-(\boldsymbol{v},\boldsymbol{K}))}{\kappa_0 v}\left\{\mathrm{Ci}(p)\sin(p) + \cos(p)\left(\tfrac{\pi}{2}-\mathrm{Si}(p)\right)\right\}, \end{aligned} \tag{47}$$

where $p = \frac{|\omega-(\boldsymbol{v},\boldsymbol{K})|}{\kappa_0 v}$ and Si and Ci are integral sine and cosine, respectively.

In what follows, to illustrate the effectiveness of the developed approach, we will apply the general theoretical results to the interpretation of experiments on the cross-correlation reflectometry in facilities for magnetic confinement of thermonuclear plasma. In this case, we will be interested in the following specification of the parameters determined by the geometry of the experiment and the expected distribution of density perturbation carriers over velocities.

When probing the radial density profile of a toroidal axisymmetric plasma, the wavelength of the injected EM field is chosen from the condition of reflection of the probing radiation from a region of dense magnetized plasma. When EM waves are injected in the electron cyclotron (EC) frequency range, EC waves are often used with the so-called ordinary polarization. In this case, the radial reflection point (more precisely, the magnetic surface on which the wave is reflected) is the point where the frequency of the injected wave coincides with the local value of the plasma frequency. Note that, in addition to reflecting the probing EM radiation while maintaining its fundamental frequency, radiation is also scattered with a relatively small change in frequency. This shift is determined primarily by the Doppler shift due to the scattering of the wave by traveling density fluctuations (see Equation (42)), which essentially coincides with the effect of the formation of a structure of the Mandelstam–Brillouin doublet type [46] in the scattering of light by sound waves in elastic media. In addition, there is a broadening of the spectrum due to the finite lifetime of the traveling density fluctuation (see broadening of the delta function due to the difference of the Holstein function from unity in Equation (40)). Taking into account the relative smallness of the deviation of the scattered radiation frequency from the frequency of the probing EM wave, $\omega_i \approx \omega_s$, we have a simple equation for the modulus of the scattering vector:

$$K = 2n\frac{\omega_i}{c}\sin\frac{\theta}{2}, \tag{48}$$

where n is the refractive index of the medium and θ is the angle between the scattered wave and the incident wave.

To implement radial reflectometry, which is of practical interest to us, it is necessary to inject and receive the reflected signal approximately perpendicular to the magnetic surfaces so that the scattering vector $\boldsymbol{K}$ in Equation (3) is directed strictly along the minor radius of the toroidal plasma column (see, for example, Figures 1–3 in [40]).

If there are several types of scatterers (density fluctuations) in the plasma with given distribution functions for the velocities $h_m(\boldsymbol{v})$ and a given relative amount A_m, then the scattering spectrum contains the sum over the types of scatterers and the averaging over the velocities for each type:

$$\frac{dW(\omega,\hat{\boldsymbol{n}},\boldsymbol{r}_1,t)}{d\Omega_{\hat{\boldsymbol{n}}}\,d\omega_s} = \sum_m A_m \int d\boldsymbol{v} h_m(\boldsymbol{v})\frac{dW_m(\omega,\hat{\boldsymbol{n}},\boldsymbol{r}_1,t,\boldsymbol{v})}{d\Omega_{\hat{\boldsymbol{n}}}\,d\omega_s}. \tag{49}$$

We will be interested in the case of two types of scatterers: traveling density fluctuations, whose velocity determines the components of the scattering spectrum with a significant shift in the relative probing frequency, and "almost standing" density fluctuations. In this case, both types of particles that scatter probing radiation have a certain "thermal" velocity distribution near the average velocity of a given type of particles.

For traveling fluctuations, we will use the distribution over the velocity vector, which has a Gaussian form:

$$h(\boldsymbol{v},\boldsymbol{v}_0,\alpha) = \left(\frac{1}{\sqrt{2\pi}\alpha v_0}\right)^3 \exp\left(-\frac{(\boldsymbol{v}-\boldsymbol{v}_0-\boldsymbol{v}_{pl})^2}{2(\alpha v_0)^2}\right), \tag{50}$$

where $\boldsymbol{v}_{pl}$ is the average mass (i.e., hydrodynamic) velocity of the plasma in the laboratory coordinate system (i.e., relative to the measuring equipment), $\boldsymbol{v}_0$ is the average velocity of fluctuations in the plasma rest frame, and α describes the width of the velocity distribution in the units of the average velocity. We will be interested in the case when the scattering vector is directed perpendicular to the velocity of the hydrodynamic motion of the plasma. Then, we can use the following distribution over velocity projections parallel to the vector $\boldsymbol{K}$:

$$h\left(v_\parallel, \pm v_{0,\parallel}, \alpha\right) = \left(\frac{1}{\sqrt{2\pi}\alpha v_{0,\parallel}}\right)^2 \exp\left(-\frac{\left(v_\parallel \pm v_{0,\parallel}\right)^2}{2\left(\alpha v_{0,\parallel}\right)^2}\right), \tag{51}$$

For almost standing fluctuations, the average velocity $v_{0,\parallel} = 0$ and the velocity distribution width is given by the average thermal velocity equal to v_T:

$$h_c\left(v_\parallel, v_T\right) = \frac{1}{\sqrt{2\pi}v_T}\exp\left(-\frac{{v_\parallel}^2}{2{v_T}^2}\right). \tag{52}$$

The distribution over the free path of such fluctuations will be considered in the diffusion model, i.e., $T(\rho) = \exp(-\kappa_0\rho)$, which gives

$$\int_0^{+\infty} dt e^{-i(\omega-(\boldsymbol{v},\boldsymbol{K}))t} T(|\boldsymbol{v}|t) = \int_0^{+\infty} dt e^{-i(\omega-(\boldsymbol{v},\boldsymbol{K}))t-\kappa_0|\boldsymbol{v}|t} = \frac{1}{\kappa_0|\boldsymbol{v}| + i(\omega - (\boldsymbol{v},\boldsymbol{K}))}. \tag{53}$$

Under the assumptions described above, the total scattering spectrum will have the form (here, some of the arguments indicated in Equation (49) are omitted):

$$\begin{aligned}\frac{dW(\omega)}{d\Omega_{\hat{\boldsymbol{n}}}\, d\omega_s} = A_{left} \int dv_\| h\left(v_\|, -v_{0,\|}, \alpha\right) \frac{dW_{left}(\omega)}{d\Omega_{\hat{\boldsymbol{n}}}\, d\omega_s} + A_{right} \int dv_\| h\left(v_\|, v_{0,\|}, \alpha\right) \frac{dW_{right}(\omega)}{d\Omega_{\hat{\boldsymbol{n}}}\, d\omega_s} \\ + A_{centr} \int dv_\| h_c\left(v_\|, v_T\right) \frac{dW_{centr}(\omega)}{d\Omega_{\hat{\boldsymbol{n}}}\, d\omega_s},\end{aligned} \tag{54}$$

where the left and right components of the spectrum correspond to the contribution of scatterers with, respectively, positive and negative values of the velocity projection onto the direction of the scattering vector, and the modules of the velocities of motion along and against the direction of the scattering vector are considered to be the same, which correspond to the motion of density fluctuations of the same type.

5. Cross-Correlation Function of Scattering

According to Equation (20), the spectrum of the cross-correlation function can be expressed in terms of the correlator of fluctuations in the density of radiation scatterers. Consider the numerator in Equation (20) in the case when there are several types of diagnostic radiation scatterers:

$$\begin{aligned}&\lim_{T_0\to\infty} \tfrac{1}{T_0} \hat{\boldsymbol{E}}^*(\boldsymbol{r}_1, \omega, \boldsymbol{K}_1)\hat{\boldsymbol{E}}(\boldsymbol{r}_2, \omega, \boldsymbol{K}_2) \\ &\quad = 2\pi[\hat{\boldsymbol{n}}_1, [\hat{\boldsymbol{n}}_1, \boldsymbol{E}_0]][\hat{\boldsymbol{n}}_2, [\hat{\boldsymbol{n}}_2, \boldsymbol{E}_0]] e^{i(\boldsymbol{K}_1,\boldsymbol{r}_1)-i(\boldsymbol{K}_2,\boldsymbol{r}_2)} \tfrac{{r_0}^2}{|\boldsymbol{r}_1||\boldsymbol{r}_2|} \\ &\quad \times \lim_{T_0\to\infty} \tfrac{1}{T_0} \sum_{m_1}\sum_{j_1} \check{g}_{m_1}{}^*\left(\boldsymbol{r}_1, \boldsymbol{K}_1, \omega, \boldsymbol{v}_{j_1}\right) \sum_{m_2}\sum_{j_2} \check{g}_{m_2}\left(\boldsymbol{r}_2, \boldsymbol{K}_2, \omega, \boldsymbol{v}_{j_2}\right).\end{aligned} \tag{55}$$

Here, "slow" spatial coordinates are introduced into the arguments of the functions $\check{f}_m$, which were previously specified but were omitted by default.

In the case of noncollective (incoherent) scattering that we are considering, the interference effects of the contributions of fluctuations of different types can be neglected. Then, we have the numerator of the expression for the spectrum of the cross-correlation function in the form:

$$\begin{aligned}&\lim_{T_0\to\infty} \tfrac{1}{T_0} \hat{\boldsymbol{E}}^*(\boldsymbol{r}_1, \omega, \boldsymbol{K}_1)\hat{\boldsymbol{E}}(\boldsymbol{r}_2, \omega, \boldsymbol{K}_2) \\ &\quad = (2\pi)^3[\hat{\boldsymbol{n}}_1, [\hat{\boldsymbol{n}}_1, \boldsymbol{E}_0]][\hat{\boldsymbol{n}}_2, [\hat{\boldsymbol{n}}_2, \boldsymbol{E}_0]] e^{i(\boldsymbol{K}_1,\boldsymbol{r}_1)-i(\boldsymbol{K}_2,\boldsymbol{r}_2)} \tfrac{{r_0}^2}{|\boldsymbol{r}_1||\boldsymbol{r}_2|} \\ &\quad \times \lim_{T_0\to\infty} \tfrac{1}{T_0} \sum_{m}\sum_{j_1} \check{g}_{m}{}^*\left(\boldsymbol{r}_1, \boldsymbol{K}_1, \omega, \boldsymbol{v}_{j_1}\right) \sum_{j_2} \check{g}_{m}\left(\boldsymbol{r}_2, \boldsymbol{K}_2, \omega, \boldsymbol{v}_{j_2}\right)\end{aligned} \tag{56}$$

Accordingly, one of the factors in the denominator equation, i.e., Equation (20), has the form:

$$\lim_{T_{01}\to\infty}\left(\frac{1}{T_{01}}\left|\hat{\boldsymbol{E}}(\omega, \boldsymbol{r}_1, \boldsymbol{K}_1)\right|^2\right) = 2\pi[\hat{\boldsymbol{n}}_1, [\hat{\boldsymbol{n}}_1, \boldsymbol{E}_0]]^2 \frac{{r_0}^2}{|\boldsymbol{r}_1|^2} \lim_{T_{01}\to\infty} \frac{1}{T_{01}} \sum_m \sum_j \left|\check{g}_m\left(\boldsymbol{r}_1, \boldsymbol{K}_1, \omega, \boldsymbol{v}_j\right)\right|^2. \tag{57}$$

Then, taking into account Equations (56) and (57), we can obtain the final expression for the spectrum of the cross-correlation scattering function (Equation (20)) in terms of the correlator of the Fourier–Laplace transforms of the scatterer density in the form

$$C(\omega,\boldsymbol{r}_1,\boldsymbol{r}_2)=\frac{[\hat{\boldsymbol{n}}_1,[\hat{\boldsymbol{n}}_1,\boldsymbol{E}_0]]}{|[\hat{\boldsymbol{n}}_1,[\hat{\boldsymbol{n}}_1,\boldsymbol{E}_0]]|}\frac{[\hat{\boldsymbol{n}}_2,[\hat{\boldsymbol{n}}_2,\boldsymbol{E}_0]]}{|[\hat{\boldsymbol{n}}_2,[\hat{\boldsymbol{n}}_2,\boldsymbol{E}_0]]|} \times\frac{e^{i(\boldsymbol{K}_1,\boldsymbol{r}_1)-i(\boldsymbol{K}_2,\boldsymbol{r}_2)}\lim\limits_{T_0\to\infty}\frac{1}{T_0}\sum_m\left[\sum_{j_1}\breve{g}_m{}^*\left(\boldsymbol{r}_1,\boldsymbol{K}_1,\omega,\boldsymbol{v}_{j_1}\right)\sum_{j_2}\breve{g}_m\left(\boldsymbol{r}_2,\boldsymbol{K}_2,\omega,\boldsymbol{v}_{j_2}\right)\right]}{\left\{\left[\lim\limits_{T_{01}\to\infty}\frac{1}{T_{01}}\sum_{m_1}\sum_{j_1}\left|\breve{g}_{m_1}\left(\boldsymbol{r}_1,\boldsymbol{K}_1,\omega,\boldsymbol{v}_{j_1}\right)\right|^2\right]\left[\lim\limits_{T_{02}\to\infty}\frac{1}{T_{02}}\sum_{m_2}\sum_{j_2}\left|\breve{g}_{m_2}\left(\boldsymbol{r}_2,\boldsymbol{K}_2,\omega,\boldsymbol{v}_{j_2}\right)\right|^2\right]\right\}^{1/2}} \tag{58}$$

Let us consider in more detail the correlator of the density of traveling fluctuations in the numerator of the spectrum of the cross-correlation function in Equation (58) in the case of weak inhomogeneity, taking into account the result for density, in Equation (40), and the finite limit in the time integral:

$$\begin{aligned}&\sum_m\sum_{j_1}\breve{g}_m{}^*\left(\boldsymbol{r}_2,\boldsymbol{K}_2,\omega,\boldsymbol{v}_{j_1}\right)\sum_{j_2}\breve{g}_m\left(\boldsymbol{r}_2,\boldsymbol{K}_2,\omega,\boldsymbol{v}_{j_2}\right)\\&=\frac{1}{4\pi}\sum_m\sum_{j_2}\breve{g}_m\left(\boldsymbol{r}_2,\boldsymbol{K}_2,\omega,\boldsymbol{v}_{j_2}\right)\sum_{j_1}Q_{eff}{}^*\left(\boldsymbol{r}_1,\boldsymbol{K}_1,i\omega,\boldsymbol{v}_{j_1}\right)\int\limits_0^{T_0}dt_1e^{i(\omega-(\boldsymbol{v}_{j_1},\boldsymbol{K}_1))t_1}T_m\left(v_{j_1}t_1,\boldsymbol{v}_{j_1},\boldsymbol{r}_1\right).\end{aligned} \tag{59}$$

Note that here the “slow” spatial variable $\boldsymbol{r}_1$ is added to the arguments of the Holstein function since the characteristic value of the absorption coefficient, κ_0, in Equation (23), depends on it.

In the case of the noncollective (incoherent, according to the generally accepted terminology [47]) scattering considered by us, the interference effects of the contributions of fluctuations of different types can be neglected. Our next key simplification of the general expressions is to take into account only those movements that correspond to the transition of the same density fluctuation from one observed point to another by free movement at a constant speed. This corresponds to taking into account only fluctuations with a velocity

$$\boldsymbol{v}_{j_1}^{(\boldsymbol{r}_{12})}=\left|\boldsymbol{v}_{j_1}^{(\boldsymbol{r}_{12})}\right|\frac{\boldsymbol{r}_1-\boldsymbol{r}_2}{|\boldsymbol{r}_1-\boldsymbol{r}_2|}. \tag{60}$$

Taking into account also the assumption about the perturbativity of the finite free path effect used in deriving Equation (45), the integral in Equation (59) can be calculated:

$$\int\limits_0^{T_0}dt_1e^{i(\omega-(\boldsymbol{v}_{j_1},\boldsymbol{K}_1))t_1}T_m\left(v_{j_1}t_1,\boldsymbol{v}_{j_1},\boldsymbol{r}_1\right)=T_0\exp\left[i\left(\omega-\left(\boldsymbol{K}_1,\boldsymbol{v}_{j_1}^{(\boldsymbol{r}_{12})}\right)\right)\Delta t_{12}{}^{(j_1)}\right]T_m\left(\left|\boldsymbol{v}_{j_1}^{(\boldsymbol{r}_{12})}\right|\Delta t_{12}{}^{(j_1)},\ \left|\boldsymbol{v}_{j_1}^{(\boldsymbol{r}_{12})}\right|\right), \tag{61}$$

where the delay time of the recorded signal for radial reflectometry is determined by the direct passage of the scattering density fluctuations between the observed points:

$$\Delta t_{12}{}^{(j_1)}=\frac{|\boldsymbol{r}_1-\boldsymbol{r}_2|}{\left|\boldsymbol{v}_{j_1}^{(\boldsymbol{r}_{12})}\right|}. \tag{62}$$

For the case of poloidal reflectometry, when the scattering vector is directed along the minor radius of the toroidal plasma column and points are observed at the same values of the minor radius and different values of the poloidal angle, at a high poloidal rotation rate (comparable to or higher than the traveling fluctuation velocity in the plasma rest frame) in the expression for the delay time of the scattered electric field, it is necessary to take into account the velocity of the poloidal hydrodynamic motion of the plasma:

$$\Delta t_{12}{}^{(j_1)}=\frac{|\boldsymbol{r}_1-\boldsymbol{r}_2|}{\left|\boldsymbol{v}_{pol}+\boldsymbol{v}_{j_1}^{(\boldsymbol{r}_{12})}\right|}. \tag{63}$$

The Holstein function takes into account only the dependence on the difference in spatial coordinates of observation points, while for the absorption coefficient in the Holstein function, we have to allow for the dependence on the velocity and may neglect the dependence on the space coordinate. Then, the correlator of the densities of traveling fluctuations for the type of particles m, which take into account the motions from point 2 to point 1, can be represented as follows:

$$\begin{aligned}&\sum_m \sum_j \breve{g}_m{}^*(\boldsymbol{r}_1, \boldsymbol{K}_1, \omega, \boldsymbol{v}_j)\breve{g}_m(\boldsymbol{r}_2, \boldsymbol{K}_2, \omega, \boldsymbol{v}_j) \\ &= \tfrac{T_0}{4\pi}\sum_m \sum_j T_m\left(\left|\boldsymbol{v}_j^{(\boldsymbol{r}_{12})}\right|\Delta t_{12}{}^{(j_1)},\ \left|\boldsymbol{v}_j^{(\boldsymbol{r}_{12})}\right|\right) \times \left|\breve{g}_m\left(\boldsymbol{r}_2, \boldsymbol{K}_2, \omega, \boldsymbol{v}_j^{(\boldsymbol{r}_{12})}\right)Q_{eff}{}^*\left(\boldsymbol{r}_1, \boldsymbol{K}_1, i\omega, \left|\boldsymbol{v}_j^{(\boldsymbol{r}_{12})}\right|\right)\right| \\ &\quad\times \exp\left[i\left(\omega - \left(\boldsymbol{K}_1, \boldsymbol{v}_j^{(\boldsymbol{r}_{12})}\right)\right)\Delta t_{12}{}^{(j_1)}\right].\end{aligned} \tag{64}$$

One of the factors in the denominator of the cross-correlation function in Equation (58) can similarly be written as

$$\sum_{j_1}\left|\breve{g}_{m_1}\left(\boldsymbol{r}_1, \boldsymbol{K}_1, \omega, \boldsymbol{v}_{j_1}^{(\boldsymbol{r}_{12})}\right)\right|^2 = \frac{T_0}{4\pi}\sum_{j_1}\left|\breve{g}_{m_1}\left(\boldsymbol{K}_1, \omega, \boldsymbol{v}_{j_1}^{(\boldsymbol{r}_{12})}\right)Q_{eff}{}^*\left(\boldsymbol{K}_1, i\omega, \left|\boldsymbol{v}_{j_1}^{(\boldsymbol{r}_{12})}\right|\right)\right|. \tag{65}$$

Then, the final result for the spectrum of the cross-correlation function with a known relative number A_m of carriers of the m-th kind takes the form:

$$\begin{aligned}C(\omega, \boldsymbol{r}_2 \to \boldsymbol{r}_1) = &\tfrac{[\hat{\boldsymbol{n}}_1,[\hat{\boldsymbol{n}}_1,\boldsymbol{E}_0]]}{|[\hat{\boldsymbol{n}}_1,[\hat{\boldsymbol{n}}_1,\boldsymbol{E}_0]]|}\tfrac{[\hat{\boldsymbol{n}}_2,[\hat{\boldsymbol{n}}_2,\boldsymbol{E}_0]]}{|[\hat{\boldsymbol{n}}_2,[\hat{\boldsymbol{n}}_2,\boldsymbol{E}_0]]|}e^{i(\boldsymbol{K}_1,\boldsymbol{r}_1)-i(\boldsymbol{K}_2,\boldsymbol{r}_2)}\sum_m A_m \\ &\times \frac{\left[\sum_j T_m\left(\left|\boldsymbol{v}_j^{(\boldsymbol{r}_{12})}\right|\Delta t_{12}{}^{(j)},\ \left|\boldsymbol{v}_j^{(\boldsymbol{r}_{12})}\right|\right)\exp\left[i\left(\omega-\left(\boldsymbol{K}_1,\boldsymbol{v}_j\right)\right)\Delta t_{12}{}^{(j)}\right]\left|g_m\left(\boldsymbol{r}_2,\boldsymbol{K}_2,\omega,\boldsymbol{v}_j^{(1,2)}\right)\right|\right]}{\left\{\left[\sum_{m_1}\sum_{j_1}\left|g_{m_1}\left(\boldsymbol{r}_1,\boldsymbol{K}_1,\omega,\boldsymbol{v}_{j_1}^{(1,2)}\right)\right|\right] \times \left[\sum_{m_2}\sum_{j_2}\left|g_{m_2}\left(\boldsymbol{r}_2,\boldsymbol{K}_2,\omega,\boldsymbol{v}_{j_2}^{(1,2)}\right)\right|\right]\right\}^{-1/2}}.\end{aligned} \tag{66}$$

It can be seen that the result explicitly depends on the Holstein function, which describes the nonlocality of the transfer process, since its deviation from the exponential dependence (in particular, a power-law decay with increasing distance) leads to a slow decay with increasing distance (in particular, to a difference in the decay of pair density correlations from exponential in the case of using a Gaussian function).

Note that here the "slow" spatial variable $\boldsymbol{r}_1$ is added to the arguments of the Holstein function, since the characteristic value of the absorption coefficient, κ_0 in Equation (23), depends on it.

Let us consider the case of radial correlation reflectometry, when we can put $\boldsymbol{K}_1 = \boldsymbol{K}_2 = \boldsymbol{K}$, and the scattering vector has only the radial component K_r. For one kind of scatterers with velocity distribution $h(\boldsymbol{v})$, from Equation (66), we obtain:

$$C(\omega, \boldsymbol{r}_2 \to \boldsymbol{r}_1) = e^{i(\boldsymbol{K},\boldsymbol{r})}\frac{\langle T(|v_r|\Delta t_{12},\ |v_r|)\exp[i(\omega - K_r v_r)\Delta t_{12}]|g(\boldsymbol{r}_2, K_r, \omega, v_r)\rangle|}{\{\langle|g(\boldsymbol{r}_1, K_r, \omega, v_r)|\rangle\ \langle|g(\boldsymbol{r}_2, K_r, \omega, v_r)|\rangle\ \}^{1/2}}, \tag{67}$$

where the angle brackets denote the averaging over the velocities along the direction of the vector $\boldsymbol{r}_1 - \boldsymbol{r}_2$ between the observation points, i.e.,

$$\langle\varphi(v_r)\rangle = \int dv_r h(v_r)\varphi(v_r), \tag{68}$$

where v_r is the radial projection of the vector in Equation (60). Note that Equation (67) shows that $C(\omega, 0) = T(0) = 1$.

From Equation (67), one can see the general physical meaning of the cross-correlation function obtained in our model: it is the result of averaging (over the spectral density of fluctuations) the product of two factors, the probability that a traveling fluctuation can freely pass (i.e., without "absorption" of a traveling fluctuation, which means the stoppage of this fluctuation in the medium) the distance between two scattering points of the probing radiation (this probability is described by the Holstein function) and the phase factor describing the phase shift of the scattered radiation due to the delay in the scattering signal for a freely moving scatterer of probing radiation (the Doppler frequency shift of the scattered radiation is also taken into account in the phase shift).

The correlation function in Equation (67) assumes the localization of the contribution of density fluctuations to the scattered radiation at a fixed frequency of the probing radiation. This assumption underlies the method of radial correlation Doppler reflectometry in tokamaks: the scanning of a probing wave in frequency corresponds to the scanning of the spatial profile of density fluctuations over the minor radius of the plasma column. However, detailed studies of the problem of wave scattering have shown the possible significant role of nonlocalized, volumetric scattering when it is necessary to take into account scattering from all points of the probing wave trajectory in plasma (see, for example, [49]). The question of the significance of volumetric scattering remains open. To solve it, it is necessary to take into account the significant nonstationarity of the cross-correlation function of the plasma density in the sense that the velocity distribution of traveling fluctuations of density may strongly influence the spectrum of the scattered electric field and the spectrum of the cross-correlation of these fields. In this paper, we restrict ourselves to the assumption of spatial localization and check the possibility of interpreting measurements in tokamaks in the standard approach to the problem of localization of the scattering region.

The cross-correlation function $C(\omega, \boldsymbol{r}_2 \to \boldsymbol{r}_1)$ (Equation (20)), for which we obtained the analytical description in Equations (66) and (67), is a complex quantity depending on the frequency and the distance between of a pair of points. When processing experimental data, it is customary to calculate the amplitude (modulus of coherence, $|C(\omega, \boldsymbol{r}_2 \to \boldsymbol{r}_1)|$) and the phase Φ (cross-phase) of the cross-correlation function shown in Equation (20):

$$\Phi = Im\,\{\ln[C(\omega, \boldsymbol{r}_2 \to \boldsymbol{r}_1)]\}. \tag{69}$$

In the case of a monochromatic distribution of fluctuations over their velocity, the derivative of the cross-phase with respect to frequency takes the form:

$$\frac{\partial \Phi}{\partial \omega} \cong \frac{|\boldsymbol{r}_1 - \boldsymbol{r}_2|}{v}. \tag{70}$$

This expression is often used to estimate the velocity of fluctuations from the slope of the curve describing the spectral dependence of the cross-phase. We note that in the case of a nonmonochromatic distribution of traveling fluctuations over velocities, such an estimate can significantly overestimate the average velocity estimate, since taking into account this nonmonochromaticity leads to the partial compensation of oscillations in Equations (66) and (67) and a decrease in the phase of the complex quantity (see the next section).

An analysis of the cross-correlation function in Equation (66) shows (see Section 6) that its difference from the exponential decay with increasing distance (in particular, from the Gaussian form) is due to the slow decay of the Holstein function. This makes it possible to explain the results of processing the measurements of the electric fields of scattered EM waves in experiments on plasma reflectometry in tokamaks (see, for example, the need to introduce a second, additional, Gaussian distribution to explain the results obtained for the cross-correlation function in Figures 5 and 6 in [40]).

6. Inverse Problem of Recovering Nonlocality Parameters of Density Fluctuation Transfer

Let us turn to the formulation and solution of the inverse problem of recovering the main characteristics of traveling and almost standing fluctuations of density from the known scattering spectrum in Equation (18) and cross-correlation function in Equation (20), based on the analytical representations in Equations (45), (49), and (66) we have obtained). We assume a strong "quenching" of almost standing fluctuations: $\sigma\tau \gg \omega\tau \gg 1$.

The sought-for parameters are as follows:

- The vector of the average velocity of traveling fluctuations v_0, which includes its projections on the scattering vector and on the direction between the observation points for cross-correlation analysis (in the case of radial correlation reflectometry;

these directions coincide and are such along the minor radius of the axially symmetric toroidal plasma);

- Width of the velocity distribution function of traveling fluctuations, α, introduced in Equation (50);
- The absorption coefficient of traveling fluctuations, κ_0, in the Holstein function Equation (23), which will be considered in the following form, which contains two sought-for parameters, $\kappa_{0,\text{res}}$ and β:

$$\kappa_0(\boldsymbol{v}) = \kappa_0(\boldsymbol{v}_0)\exp\left(\frac{(\boldsymbol{v}-\boldsymbol{v}_0)^2}{(\beta\boldsymbol{v}_0)^2}\right) \equiv \kappa_{0,\text{res}}\exp\left(\frac{(\boldsymbol{v}-\boldsymbol{v}_0)^2}{(\beta\boldsymbol{v}_0)^2}\right), \tag{71}$$

- The decay rate of the Holstein function Equation (23), γ, describing the degree of nonlocality of the transfer of density fluctuations;
- The average "thermal" velocity of almost standing density fluctuations, v_T, that describes the width of the velocity distribution and plays a role similar to the parameter α introduced above for traveling fluctuations;
- Absorption coefficient for almost standing density fluctuations, $\kappa_{0,\text{c}}$, when specifying the Holstein function in the form $T_\text{c}(\rho) = \exp(-\kappa_{0,\text{c}}\rho)$ for almost standing fluctuations;
- The relative number (weight) of traveling fluctuations whose velocities are directed along the direction to the observer (see Figures 1–3 in [40]), A_{right}, and in the opposite direction, A_{left}, as well as almost standing fluctuations, A_{centr}.

When solving the inverse problem, it is assumed that the mean free path of traveling density fluctuations is much larger than that of almost standing fluctuations, i.e., $\kappa_{0,\text{c}} \gg \kappa_0$.

In the turbulence models previously used to interpret the measurement results (see, for example, the formula on p. 449 [40]), there were sought-for parameters that are also present in our model, namely:

- Average lifetime of density fluctuations τ (note that the lifetime distribution function is taken as exponential, which is also done in our model);
- Average velocity of traveling fluctuations $\boldsymbol{v}_0$;
- The mean free path of traveling fluctuations $1/\kappa_0$, which determines the decay of the cross-correlation function.

We have added the following important parameters, which became possible due to the solution of the kinetic equation for density fluctuations:

- The width of the distribution function around the average velocity of the density fluctuations (e.g., the width of the Gaussian velocity distribution, i.e., the effective temperature of the density fluctuations). This value contributes to the width of the side components of the spectral intensity of the scattered radiation in the Mandelstam–Brillouin doublet (this corresponds to the introduction of the parameter α);
- The width of the free path distribution function (this corresponds to the parameter γ in the Holstein function).

In what follows, we take the quenching parameter $\sigma\tau = 20$, which is the ratio of the average lifetime of standing fluctuations to the average time of their disappearance, and not of their transformation into traveling fluctuations. This choice corresponds to the thermodynamic limit of the effective source of standing fluctuations (Equation (41)). Actually, this parameter and the entire effective source drop out of the cross-correlation function due to its cancellation in the numerator and denominator, since we assume a weak dependence of the effective source on phase-space variables compared with the Fourier–Laplace transforms of plasma density fluctuations. The very idea of the cross-correlation function is to minimize its dependence on the source of the studied carriers and maximize its dependence on kinematic, traveling properties of carriers.

Next, we consider the application of the proposed algorithm to the interpretation of the results of measurements on the T-10, TEXTOR, and ASDEX tokamaks.

6.1. T-10 Tokamak

When solving the inverse problem of recovering the characteristics of density fluctuations from the experimental data of reflectometry on the T-10 tokamak (Figure 4a,b in [40]), it is possible to determine the numerical values of parameters.

(1) The fixed input parameter, i.e., the modulus of the scattering wave vector, $\boldsymbol{K}$ (Equation (48)): It is specified by the geometry of the diagnostics, while the value of the refractive index is taken close to unity, taking into account density fluctuations near the surface on which the probing waves are reflected. For T-10 tokamak case [40], we take $K = 16.3\ \text{cm}^{-1}$.

(2) The parameters found at the first stage of optimization from the position of the maxima of the quasi-coherent components in the scattering spectrum: the average values of the longitudinal (i.e., radial) $v_{0,\|}$ and transverse $v_{0,\perp}$ (with respect to the scattering vector) velocities of traveling fluctuations: $v_{0,\|} = v_{0,\perp} = 4.2 \times 10^4$ cm/s.

It is important to note that the accuracy of estimating the modulus of the scattering vector is limited by the fact that the refractive index at the reflection point (cut-off) of the O-wave generally vanishes and it is necessary to solve the wave problem of reflection from the plasma layer with considerable density fluctuations. In addition, segments on the way to cut-off can make a significant contribution to scattering. Therefore, strictly speaking, from the position of the peaks in the Mandelstam–Brillouin doublet, one can only find the product of the scattering vector and the average velocity of traveling density fluctuations. However, even under conditions of limited accuracy in the reconstruction of these parameters, it is possible to obtain reasonable estimates of the required degree of nonlocality of the transfer of density fluctuations.

(3) Optimized parameters (i.e., found by solving the inverse problem): $A_{left} = 0.01$, $A_{right} = 0.013$, $A_{centr} = 0.01$, $\alpha = 0.458$, $v_T = 10^4$ cm/s, $v_{pol} = 2.0 \times 10^4$ cm/s, $\kappa_{0,res} = 0.3\ \text{cm}^{-1}$, $\beta = 1$, $\kappa_{0,centr} = 10\ \text{cm}^{-1}$, and $\gamma = 0.55$, where v_{pol} is the velocity of the poloidal rotation of plasma.

The results of reconstruction and comparison of the experimental and calculated theoretical curves are shown below, in Figures 1–4.

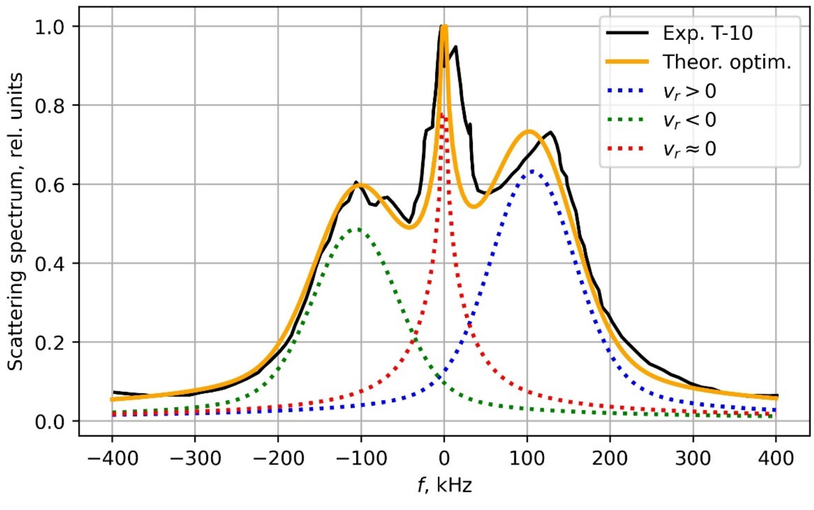

Figure 1. Spectrum of radiation scattered by traveling and almost standing density fluctuations: experimental spectrum from Figure 4a [40] (black curve), the result of the best fitting of this spectrum calculated by Equations (49) and (45) (orange curve). The individual components of the spectrum are shown: the contributions of nearly standing fluctuations (red dotted line) and radially traveling fluctuations from the observation point to the observer (blue dotted line) and in the opposite direction (green dotted line). Discharge parameters: current $I = 160$ kA, magnetic field $B = 2.5$ T, and electron density $n_e = 1.2 \times 10^{13}\ \text{cm}^{-3}$. The radial coordinate of the reflection point of the probing beam is $r = 19.5$ cm (presumably, the scattering point of the probing wave).

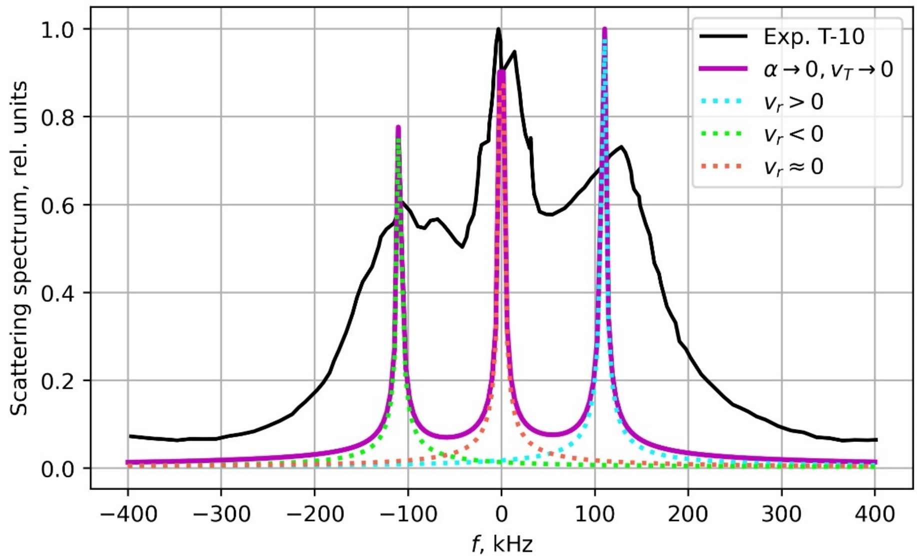

Figure 2. Scattered radiation spectrum with a monochromatic distribution of traveling and almost standing density fluctuations over velocities (lilac curve) (Equations (49) and (45)) in comparison with the experimental spectrum from Figure 4a [40] (black curve). Individual components of the spectrum are shown: the contribution of almost standing fluctuations (red dotted line) and radially travelling fluctuations from the observation point to the observer (blue dotted line) and in the opposite direction (green dotted line). The discharge parameters are the same as those shown in Figure 1.

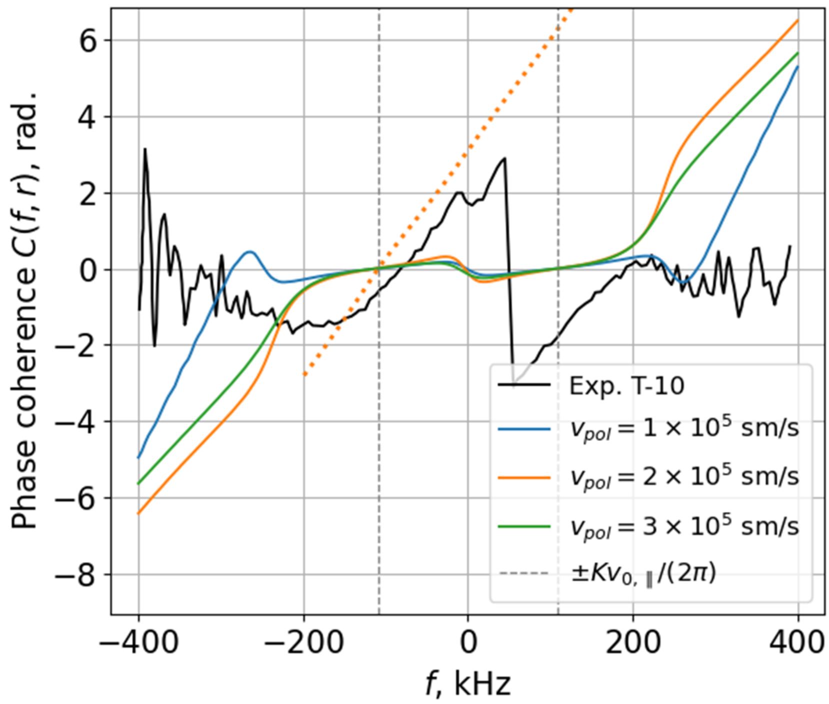

(**a**)

Figure 3. *Cont.*

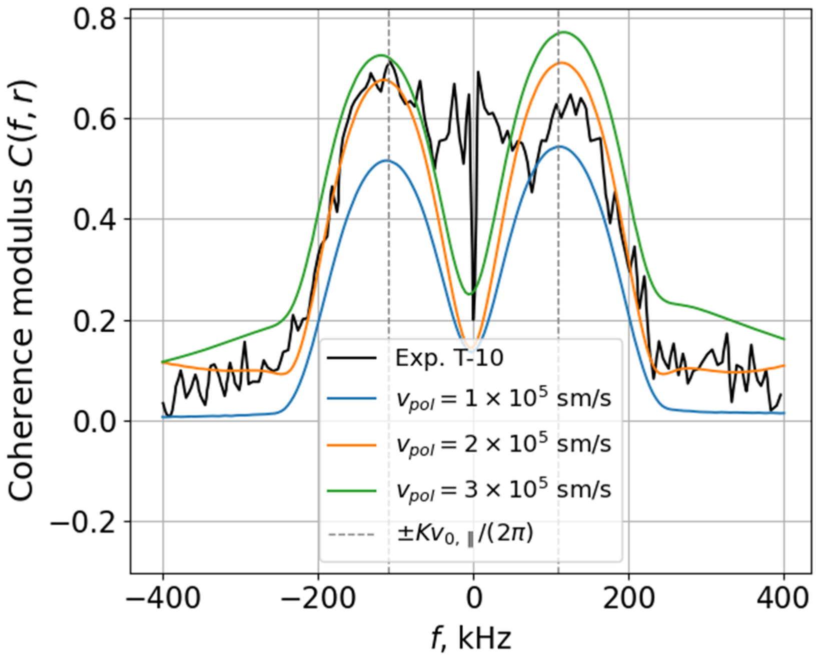

(**b**)

Figure 3. Comparison of the calculations of the cross-correlation function (Equation (66)) for poloidal correlations, with the optimal values found when fitting the experimental data for the scattering spectrum and the radial coordinate dependence of the cross-correlation function (the results of the fitting are shown in Figures 1 and 4a,b). (**a**) Coherence phase (Equation (69)); (**b**) modulus of coherence, which is the modulus shown in Equation (66), as a function of frequency for three different values of the plasma poloidal rotation velocity v_{pol}. The orange dotted curve corresponds to the case of a monochromatic distribution of density fluctuations over their velocities for the optimal value of v_{pol}. Dashed vertical lines show the position of the peaks of the theoretical curves in Figure 1 corresponding to the optimal value of the average velocity of traveling density fluctuations. The black curve is experimental [40]: (**a**) Figure 4b and (**b**) Figure 4c in Ref. [40]. The discharge parameters coincide with those shown in Figure 1. The radial coordinate of two reflection points of the probing beam is 19.5 cm (presumably, the scattering point of the probing wave), and the poloidal distance between reflection points is 1 cm.

Figure 1 shows that the side components of the scattering spectrum (at a frequency $\omega/2\pi \approx \pm 110$ kHz), which are called quasi-coherent oscillations [41–43], can be interpreted as a Mandelstam–Brillouin doublet in light scattering in an elastic medium. Therefore, from the location of the peak and the width of the spectrum of scattered radiation, one can (by solving the inverse problem) find the value of the projection of the average velocity of fluctuations in the direction of the scattering vector $\boldsymbol{K}$ (with the reservation indicated above) and the dispersion of the velocity of traveling fluctuations described by the parameter α.

To illustrate the relative role of different mechanisms of spectrum broadening in quasi-coherent components, Figure 2 shows the spectra for a monochromatic velocity distribution of density fluctuations. It can be seen that the broadening due to the finite length of the free path is much smaller than the "thermal" broadening of traveling fluctuation velocity, which is determined by the width of their velocity distribution.

The results of solving the inverse problem for the cross-correlation function for the problem of reflectometry at the T-10 tokamak [40] are shown below. Figure 3 shows the spectral distribution for a fixed distance between two points with the same minor radius coordinate and different poloidal coordinates. Figure 3a shows that the slope of the calculated phase in the region of the spectrum of each quasi-coherent component (left or right) significantly differs from that of the experimental curve, while the slope of the theoretical curve for the optimal value of poloidal rotation velocity v_{pol} approximately coincides with the experimental one only outside these regions. At the same time, by varying v_{pol}, it is possible to obtain good agreement between the theoretical and experimental results for the modulus of the cross-correlation function, which is shown in Figure 3b (the modulus of the complex function of pair correlations is often called the coherence function). Figure 3a also shows a comparison of theoretical calculations for two different velocity distribution functions of density fluctuations, monochromatic and Gaussian, with the width obtained by solving the inverse problem of fitting experimental data for the scattered radiation spectrum shown in Figure 1.

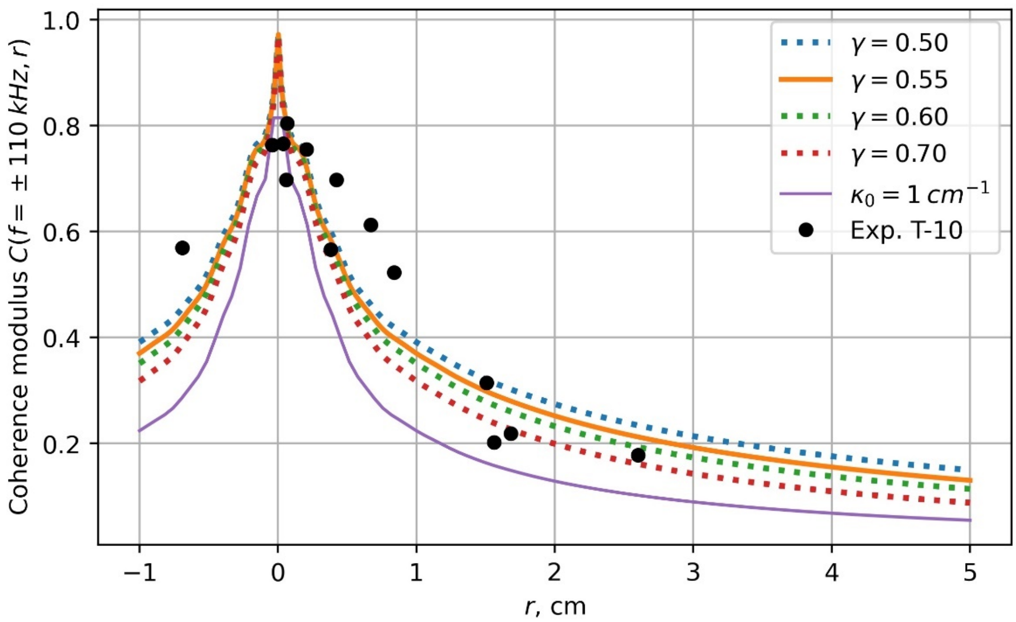

(**a**)

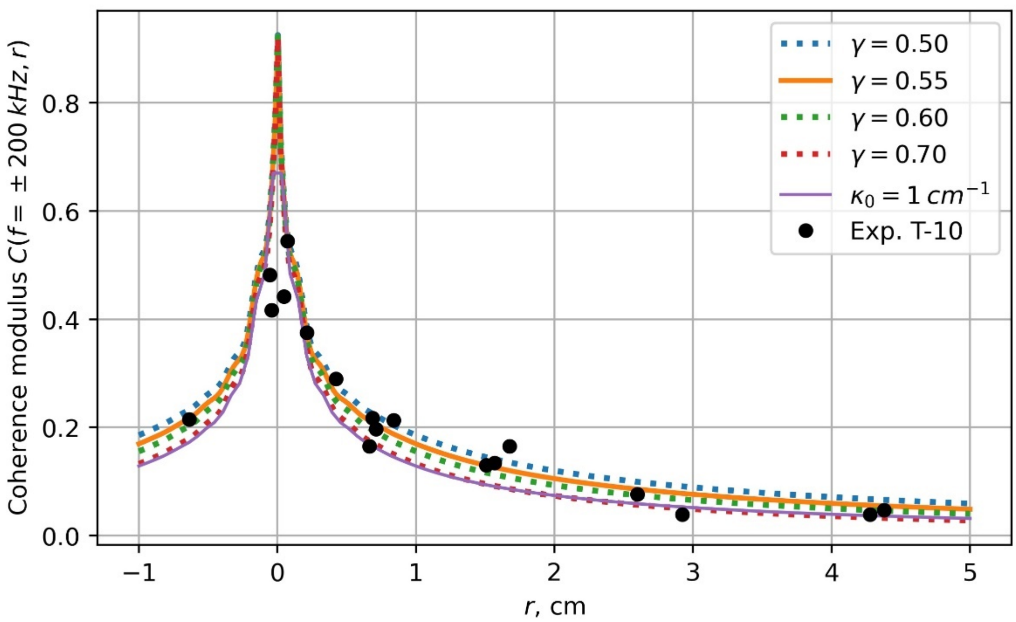

(**b**)

Figure 4. *Cont*.

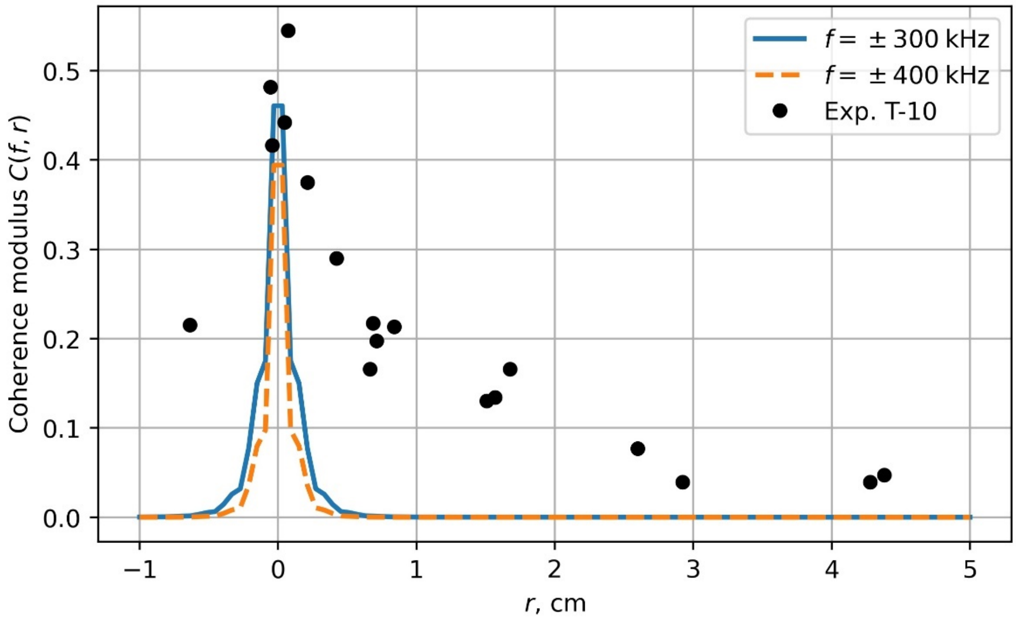

(**c**)

Figure 4. Coordinate dependence of the modulus of the cross-correlation function (Equation (66)) (coherence modulus) for the frequencies (**a**) $f = \pm 110$ kHz and (**b**) $f = \pm 200$ kHz for different values of the parameter γ: $\gamma = 0.5$ (dashed blue line), $\gamma = 0.55$ (orange curve), $\gamma = 0.6$ (green dotted line), and $\gamma = 0.7$ (red dotted line). The purple curve in figures (**a**) and (**b**) was calculated at $\varkappa_0 = 1$ cm^{-1} in the Holstein function (Equation (23)) and the rest of the curves for the dependence of the absorption coefficient on the velocity according to Equation (71). Black dots are experimental values: (**a**) quasi-coherent oscillations—Figure 5a [40]; (**b**,**c**) broadband oscillations—Figure 5b [40]. (**c**) shows the coherence modulus for frequencies $f = \pm 300$ kHz (blue curve) and $f = \pm 400$ kHz (orange dotted line). Discharge parameters: current $I = 140$ kA, magnetic field $B = 2.5$ T, and electron density $n_e = 1.2 \times 10^{13}$ cm^3. The radial coordinate is counted from the point of reflection of the probing beam $r = 10$ cm (presumably, the scattering point of the probing wave).

A comparison of the theoretical and experimental cross-correlation functions as functions of the radial distance between two points with the same poloidal coordinate for different fixed frequencies of the scattered radiation is shown in Figure 4. In addition, the results in Figure 4a show a comparison of theoretical curves for different values of the nonlocality parameter, γ, to illustrate the sensitivity of the optimization result to this parameter. For broadband oscillations with a frequency $f = \pm 200$ kHz, the possibility of excellent agreement between the model radial correlation function and the experimental data is shown (Figure 4b). For high frequencies (Figure 4c), one can see a rapid damping of the calculated curve. This comparison for various frequencies shows the range of the applicability of our model for the quasi-coherent mode to the description of experimental data: for the center of the quasi-coherent mode (Figure 4a) and the wings of this mode (Figure 4b), the agreement is good, whereas for larger detuning from the center of the quasi-coherent mode, there is no agreement.

The results presented in Figures 1–4 are the first attempt in the literature to simultaneously interpret poloidal and radial correlation reflectometry data by solving a unified inverse problem for the cross-correlation function as a function of two variables, the frequency of the scattered electric field and the spatial coordinate. The agreement between the theoretical and experimental results is good, except for the phase of the cross-correlation function. The latter can be partially explained by the difficulty of studying this characteristic both in theory and in experiment. In particular, the error in determining the phase of a complex function increases with a decrease in the modulus of the function.

6.2. TEXTOR Tokamak

In the TEXTOR tokamak, poloidal correlations of plasma density fluctuations have been studied [50]: the observation points were located on the same minor radius coordinate (the same magnetic surface) and at different poloidal angles within this magnetic surface. In this case, one has to take into account the poloidal hydrodynamic motion with the delay (Equation (63)) in the cross-correlation function (Equations (66) and (67)). Solving the inverse problem of restoring the characteristics of density fluctuations from the experimental data of reflectometry on the TEXTOR tokamak (Figure 3a,b in [50]), one can similarly determine the numerical values of the following parameters:

(1) Fixed input parameters: $K = 10\ \text{cm}^{-1}$. The poloidal distance between reflection points of the probing radiation along the magnetic surface is 8 cm. The following parameters were taken equal to those in the T-10 tokamak due to the closeness of the experiment geometry and discharge parameters: $\kappa_{0,res} = 0.3\ \text{cm}^{-1}$, $\beta = 1$, $\kappa_{0,centr} = 1\ \text{cm}^{-1}$, and $\gamma = 0.55$.

(2) The parameters found at the first stage of optimization from the position of the maxima of the quasi-coherent components in the scattering spectrum: the average values of the longitudinal (i.e., radial) $v_{0,\|}$ and transverse $v_{0,\perp}$ (with respect to the scattering vector) velocities of traveling fluctuations of scatterers: $v_{0,\|} = v_{0,\perp} = 6.45 \times 10^4\ \text{cm/s}$.

(3) Optimized parameters (i.e., found by solving the inverse problem): $A_{left} = 0.03$, $A_{right} = 0.03$, $A_{centr} = 0.12$, $\alpha = 0.2$, $v_T = 10^3\ \text{cm/s}$, and plasma poloidal rotation velocity $v_{pol} = 3 \times 10^5\ \text{cm/s}$.

The results of reconstruction and comparison of the experimental and calculated theoretical curves are presented below, in Figures 5 and 6. It can be seen from Figure 6a that the cross-phase slope upon averaging over frequency in the spectral range of the respective Mandelstam–Brillouin component is close enough to the experimental one and the coherence in Figure 6b qualitatively reproduces the main features of the experimental curve.

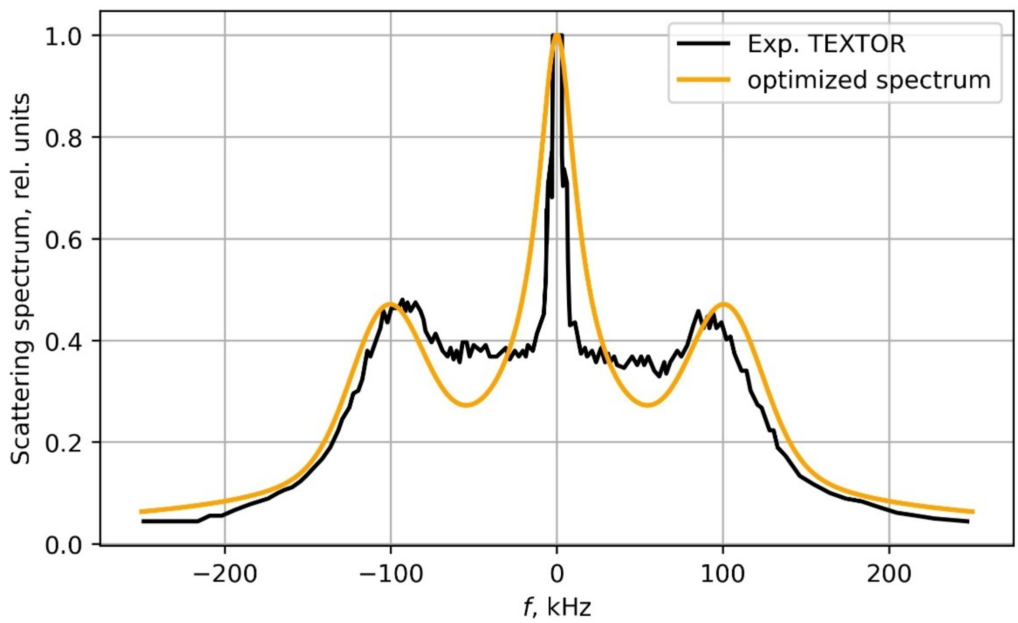

Figure 5. Spectrum of radiation scattered by traveling and almost standing density fluctuations: experimental spectrum (Figure 3a in [50]) (black curve) and the result of the best fitting of this spectrum (orange curve), calculated by Equations (49) and (45).

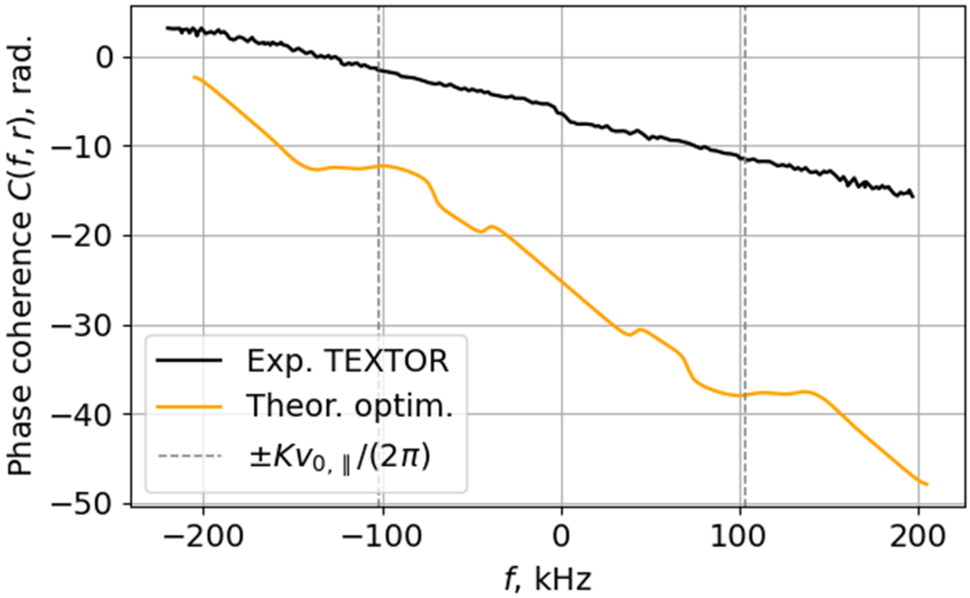

(**a**)

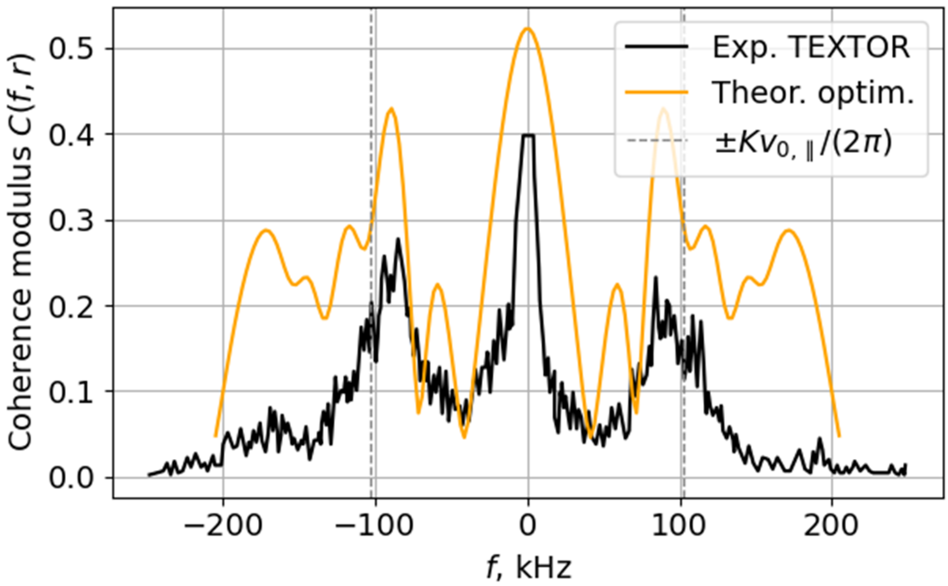

(**b**)

Figure 6. Comparison of calculations of the cross-correlation function (Equations (20) and (66)) with the found optimal values when fitting the experimental data for the scattering spectrum. (**a**) Cross-phase (Equation (69)); (**b**) modulus in Equation (66) as a function of frequency. The black curve is the experimental one [50] ((**a**) Figure 3b and (**b**) Figure 3c). The orange curve is the result of simulation using the parameter values from the best fitting of the scattering spectrum in Figure 5. Dashed vertical lines show the position of the peaks of the theoretical curve in Figure 5 corresponding to the optimal value of the average velocity of traveling density fluctuations.

A comparison of theoretical and experimental data shows, as in the case of the T-10 tokamak, a partial agreement. The theoretical curve for the modulus of the cross-correlation function reproduces not only the position of the central peak of the quasi-coherent mode (QCM) components for fluctuations radially moving along and against the scattering vector but also a modulation of the smooth line shape of the QCM, which can be seen on the theoretical curve. This means that the modulation of the frequency dependence of the cross-correlation function, explicitly represented in our final analytic results, i.e., Equations (66) and (67), works well enough. The theoretical phase is close to the experiment only after averaging the slope of the spectrum over the entire region of the left or right QCM line shape component, and the reasons for the difference can be the same as in the case of the T-10 tokamak.

6.3. ASDEX Tokamak

The study of poloidal correlations of plasma density fluctuations in the ASDEX tokamak has been carried out at a given poloidal tilt of the probing radiation horns (see Figure 1 in [51,52]); therefore, Doppler frequency shifts are clearly visible in the experimental spectra (see Figure 5c in [51] and Figure 2a in [52]). However, such spectra have insufficient resolution, due to which it is not possible to single out the fine structure of the spectrum unambiguously. Despite this, it is possible to conduct a qualitative assessment of the experimental results. Figure 2a in [52] clearly shows a characteristic shift to the left by ~1 MHz due to the poloidal rotation of the plasma, with maxima ±200 kHz to the left and to the right with respect to the poloidal rotation Doppler shift.

Figure 7a shows the result of restoring the modulus of the cross-correlation function for the same parameter values as for the T-10 tokamak, but for $K = 25.6\ \text{cm}^{-1}$, which in ASDEX is different from the T-10 case because of the difference of the probing wavelength. It can be seen that at $r = 0.5$ cm, we have a qualitative agreement with local quasi-coherent maxima. Figure 7b shows the coordinate dependence of the cross-correlation function for various values of the parameter γ at a frequency $f = \pm 200$ kHz relative to a frequency shift of ~1 MHz, which corresponds to quasi-coherent oscillations.

The good agreement of the theoretical curve for the radial dependence of the cross-correlation function at the largest distances where this dependence was measured (0.5–1 cm) shows that the developed approach makes it possible to reproduce that part of the radial dependence that is most difficult to reproduce using theoretical models without taking into account the effects of nonlocality. Indeed, even for a simple fitting of such long-tailed, non-exponential functions, one has to introduce two Gaussians, associated with local rather than superdiffusion transport (see the captions for Figures 5 and 6 in [40]).

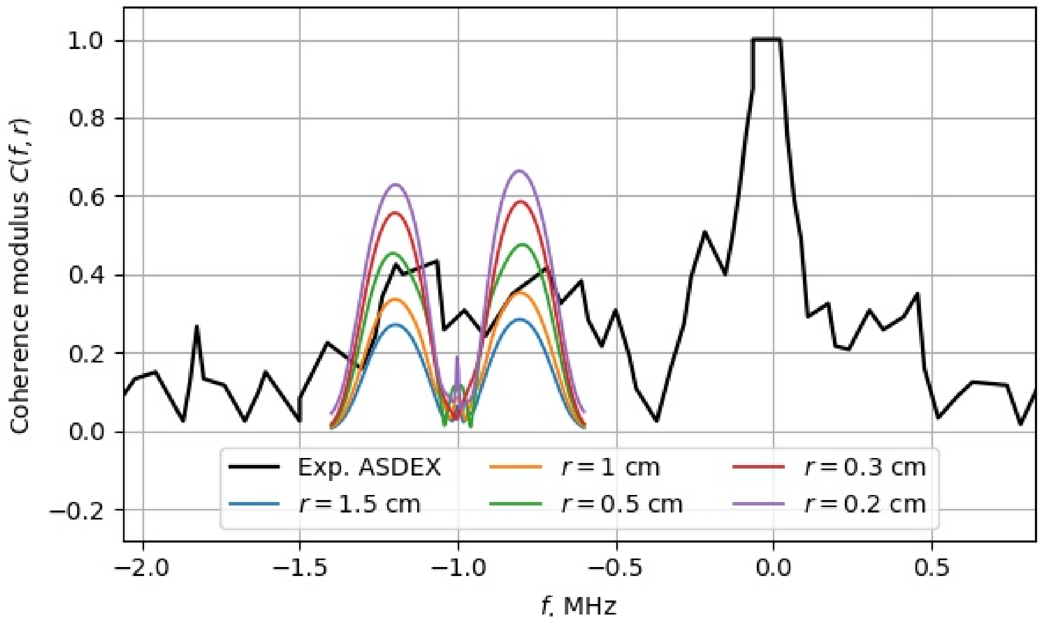

(**a**)

Figure 7. *Cont.*

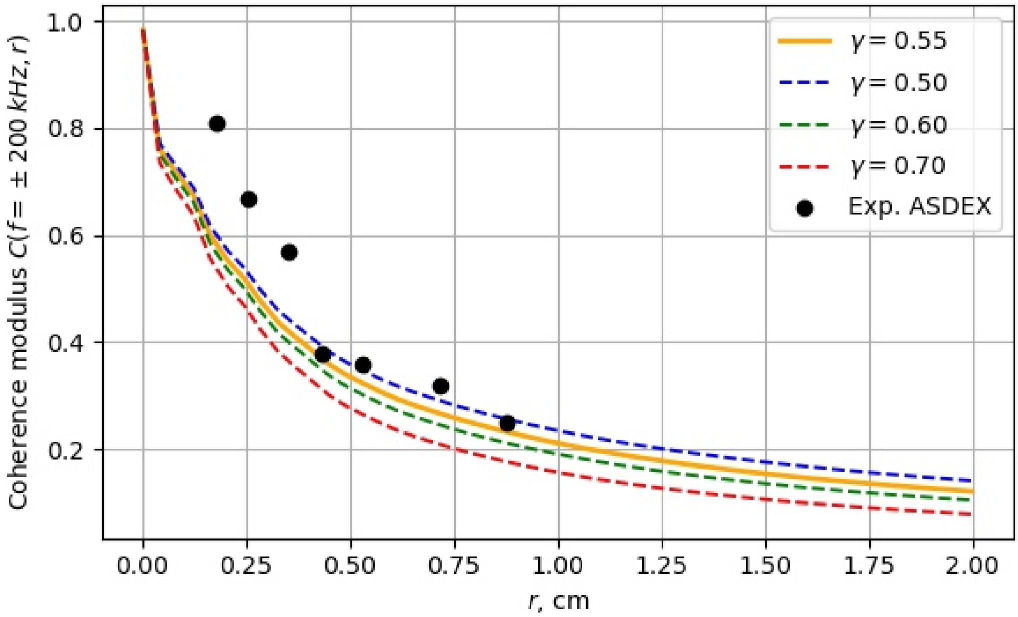

(**b**)

Figure 7. Modulus of the cross-correlation function (coherence) (Equations (20) and (66)) as a function of frequency for $r = |\boldsymbol{r}_1 - \boldsymbol{r}_2| = 1.5$ cm (blue curve), $r = 1$ cm (orange curve), $r = 0.5$ cm (green curve), $r = 0.3$ cm (red curve), and $r = 0.2$ cm (violet curve). The black curve is experimental [52]. (**b**) Coordinate dependence of the cross-correlation function (coherence) (Equations (20) and (66)) for the frequency of quasi-coherent oscillations $f = \pm 200$ kHz for $\gamma = 0.55$ (orange curve), $\gamma = 0.5$ (blue dashed line), $\gamma = 0.60$ (green dashed line), and $\gamma = 0.70$ (red dashed line). The orange curve is the result of simulation with the same parameter values as in Figure 7a for $\kappa_{0,\mathrm{res}} = 1\ \mathrm{cm}^{-1}$. The black dots are experimental [52].

7. Conclusions

This work is devoted to the application of the superdiffusion formalism to describe the kinetics of moving density fluctuations in a turbulent medium and to the formulation of an algorithm for reconstructing the nonlocal properties of stochastic processes in a medium from the spectrum of its density fluctuations, diagnosed from the scattering spectra of electromagnetic (EM) waves in the medium. The developed approach is based on the application of the concept of Lévy walks to the description of nonlocal properties of fluctuations in the density of a turbulent medium. This approach makes it possible to determine these properties from the scattering spectra of EM waves and cross-correlation reflectometry. A system of equations for density fluctuations is proposed, which is reduced to an integral equation for the pair correlation function of plasma density fluctuations. This equation is expressed in terms of the Holstein functional, which is characteristic of a wide range of nonlocal transfer processes, including the transfer of resonant radiation in plasma and gases in the Biberman–Holstein model. A universal description is obtained of the relationship between the quasi-coherent component observed in tokamaks in the spectrum of scattered EM waves in plasma and the Mandelstam–Brillouin scattering process. It is shown that the nonlocality of spatial correlations in a turbulent medium is due to long-range carriers of medium fluctuations, for which the distribution function over the free path length is described by the Lévy distribution. The effectiveness of the proposed method is shown by the example of the interpretation of the data of radial and poloidal correlation reflectometry of EM waves of the radio frequency range for the diagnostics of turbulent plasma in the T-10, TEXTOR, and ASDEX tokamaks.

Note that the value of the parameter $\gamma = 0.55$ found via solving an inverse problem for the degree of nonlocality of the transfer of radially traveling plasma density fluctuations in the T-10 tokamak is close enough to the value of the analogous parameter $\gamma \approx 2/3$ in the empirical $t^{3/2}$ Richardson law for the dynamics of the perturbation front in the medium from an instant point source in the case of hydrodynamic turbulence (such a value of the parameter γ in the Richardson law follows from (7.7) and (7.8) in [31]). This is an argument in favor of the fact that the observed density fluctuations may be of turbulent origin.

We also note that the quasi-coherent component in the spectrum can be considered not as the motion of density fluctuations in the plasma rest frame (which is accepted in our approach) but as a result of scattering of probing EM radiation by density fluctuations, which can be considered static, i.e., standing in the rest frame of the plasma, and moving relative to the receiver of the reflected radiation only due to the toroidal and poloidal rotation of the plasma as a whole, i.e., the hydrodynamic motion of plasma in a tokamak. In this case, at the point of observation identified by the signal reception conditions under the assumption that the probing radiation is scattered locally, there will also be a radial motion of the plasma forward and backward with the same velocity relative to the radiation receiver. In this case, the radial correlation will reflect the correlation of the spatial structure, which is static in the rest frame of plasma, and in fact also characterizes the formation (transfer) of perturbations in the radial direction, without which the existence of such a correlation would be impossible. Therefore, in any case, the model we propose describes the correlation properties of plasma density fluctuations and allows one to estimate the degree of nonlocality of bonds in plasma.

In conclusion, we note that the present work is the result of applying a general theoretical approach [28–33] to the practical problem of controlled thermonuclear fusion and demonstrates the relevance of the development of analytical approaches in the theory of nonlocal transfer (a modern review of the status and history of analytical approaches related to the theory of nonlocal transfer of radiation can be found in [53]).

Author Contributions: Conceptualization, A.B.K.; software and visualization, A.A.K.; methodology, formal analysis, and writing—review and editing, all co-authors. All authors have read and agreed to the published version of the manuscript.

Funding: This work was supported in part by the Russian Foundation for Basic Research: project no. 19-32-90281.

Institutional Review Board Statement: Not applicable.

Informed Consent Statement: Not applicable.

Data Availability Statement: Not applicable.

Acknowledgments: The authors are grateful to V.A. Vershkov and D.A. Shelukhin for discussing the results of measurements on tokamaks and this work and to V.S. Neverov for discussing methods for the numerical calculation of the Fourier transforms. This work has been carried out using computing resources of the federal collective usage center Complex for Simulation and Data Processing for Mega-science Facilities at NRC "Kurchatov Institute"; http://ckp.nrcki.ru/ (accessed on 30 April 2022).

Conflicts of Interest: The authors declare no conflict of interest.

References

1. Mandelbrot, B.B. *The Fractal Geometry of Nature*; W. H. Freeman: New York, NY, USA, 1982; ISBN 0-7167-1186-1189.
2. Shlesinger, M.; Zaslavsky, G.M.; Frisch, U. (Eds.) *Lévy Flights and Related Topics in Physics*; Springer: Berlin/Heidelberg, Germany, 1995; ISBN 978-3-662-14048-2.
3. Dubkov, A.A.; Spagnolo, B.; Uchaikin, V.V. Lévy flight superdiffusion: An introduction. *Int. J. Bifurc. Chaos* **2008**, *18*, 2649–2672. [CrossRef]
4. Klafter, J.; Sokolov, I.M. Anomalous diffusion spreads its wings. *Phys. World* **2005**, *18*, 29–32. [CrossRef]
5. Eliazar, I.I.; Shlesinger, M.F. Fractional motions. *Phys. Rep.* **2013**, *527*, 101–129. [CrossRef]
6. Shlesinger, M.F.; Klafter, J.; Wong, Y.M. Random walks with infinite spatial and temporal moments. *J. Stat. Phys.* **1982**, *27*, 499–512. [CrossRef]
7. Zaburdaev, V.Y.; Chukbar, K.V. Enhanced super diffusion and finite velocity of Lévy flights. *JETP* **2002**, *94*, 252–259. [CrossRef]
8. Zaburdaev, V.Y.; Chukbar, K.V. Memory effects in stochastic transport. *JETP Lett.* **2003**, *77*, 551–555. [CrossRef]
9. Zaburdaev, V.; Denisov, S.; Klafter, J. Lévy walks. *Rev. Mod. Phys.* **2015**, *87*, 483. [CrossRef]
10. Mihalas, D. *Stellar Atmospheres*; Freeman: San Francisco, CA, USA, 1970; 399p.

11. Ivanov, V. *Transfer of Radiation in Spectral Lines*; NBS Special Publication no 385; US Govt Printing Office: Washington, DC, USA, 1973.
12. Minin, I.N. *The Theory of Radiation Transfer in the Planet Atmospheres*; Nauka: Moscow, Russia, 1988; 263p. (In Russian)
13. Grinin, V.P.; Harutyunian, H.; Il'in, V.B.; Kholtygin, A.F.; Nikoghossian, A. Radiation Mechanisms of Astrophysical Objects: Classics Today. In Proceedings of the Conference in Honor of the 100th Birthday of Academician, V.V. Sobolev, St. Petersburg, Russia, 21–25 September 2015; Erevan, Edit Print. p. 435.
14. Kukushkin, A.B.; Lisitsa, V.S.; Savel'ev, Y.A. Nonlocal transport of thermal perturbations in a plasma. *JETP Lett.* **1987**, *46*, 448–451. Available online: http://www.jetpletters.ru/ps/1232/article_18610.pdf (accessed on 30 April 2022).
15. Biberman, L.M. On the diffusion theory of resonance radiation. *Sov. Phys. JETP* **1949**, *19*, 584–603.
16. Holstein, T. Imprisonment of resonance radiation in gases. *Phys. Rev.* **1947**, *72*, 1212–1233. [CrossRef]
17. Biberman, L.M.; Vorob'ev, V.S.; Yakubov, I.T. *Kinetics of Nonequilibrium Low Temperature Plasmas*; Consultants Bureau: New York, NY, USA, 1987; ISBN 978-1-4684-1667-1.
18. Veklenko, B.A. Green's function for the resonance radiation diffusion equation. *Sov. Phys. JETP* **1959**, *9*, 138–142.
19. Kogan, V.I. A Survey of Phenomena in Ionized Gases (Invited Papers). In Proceedings of the ICPIG'67, Vienna, Austria, 27 August–2 September 1968; p. 583. (In Russian)
20. Abramov, V.A.; Kogan, V.I.; Lisitsa, V.S. Radiative Transfer in Plasmas. In *Reviews of Plasma Physics*; Leontovich, M.A., Kadomtsev, B.B., Eds.; Consultants Bureau: New York, NY, USA, 1987; Volume 12, p. 151.
21. Kogan, V.I. *Encyclopedia of Low Temperature Plasma. Introduction Volume*; Fortov, V.E., Ed.; Nauka/Interperiodika: Moscow, Russia, 2000; Volume 1, p. 481. (In Russian)
22. Biberman, L.M. Approximate method of describing the diffusion of resonance radiation. *Dokl. Akad. Nauk. SSSR Ser. Phys.* **1948**, *59*, 659.
23. Kalkofen, W. (Ed.) *Methods in Radiative Transfer*; Cambridge University Press: Cambridge, UK, 1984; ISBN 0-521-25620-8.
24. Rybicki, G.B. Escape Probability Methods. In *Methods in Radiative Transfer*; Kalkofen, W., Ed.; Cambridge University Press: Cambridge, UK, 1984; Chapter 1; ISBN 0-521-25620-8.
25. Biberman, L.M.; Vorob'ev, V.S.; Lagar'kov, A.N. Radiative transfer in ionization continuum. *Opt. Spectrosc.* **1965**, *19*, 326. (In Russian)
26. Napartovich, A.P. On the τ_{eff} method in the radiative transfer theory. *High Temp.* **1971**, *9*, 23–26.
27. Starostin, A.N. *Encyclopedia of Low Temperature Plasma. Introduction Volume*; Fortov, V.E., Ed.; Nauka/Interperiodika: Moscow, Russia, 2000; Volume 1, p. 471. (In Russian)
28. Kukushkin, A.B.; Sdvizhenskii, P.A. Automodel solutions for Lévy flight-based transport on a uniform background. *J. Phys. A Math. Theor.* **2016**, *49*, 255002. [CrossRef]
29. Kukushkin, A.B.; Kulichenko, A.A. Automodel solutions for superdiffusive transport by Lévy walks. *Phys. Scripta* **2019**, *94*, 115009. [CrossRef]
30. Kulichenko, A.A.; Kukushkin, A.B. Superdiffusive transport based on Lévy walks in a homogeneous medium: General and approximate self-similar solutions. *J. Exp. Theor. Phys.* **2020**, *130*, 873–885. [CrossRef]
31. Kukushkin, A.B.; Kulichenko, A.A.; Sokolov, A.V. Similarity laws for the green function of the nonstationary super diffusive transport: Levy walks and Levy flights. *J. Exp. Theor. Phys.* **2021**, *132*, 865–881. [CrossRef]
32. Kulichenko, A.A.; Kukushkin, A.B. Super diffusive transport of Biberman-Holstein type for a finite velocity of carriers: General solution and the problem of automodel solutions. *Int. Rev. Atom. Mol. Phys.* **2017**, *8*, 5–14. Available online: https://www.auburn.edu/cosam/departments/physics/iramp/8_1/Kulichenko_Kukushkin.pdf (accessed on 30 April 2022).
33. Kukushkin, A.B.; Kulichenko, A.A.; Neverov, V.S.; Sdvizhenskii, P.A.; Sokolov, A.V.; Voloshinov, V.V. Self-similar solutions in the theory of nonstationary radiative transfer in spectral lines in plasmas and gases. *Symmetry* **2021**, *13*, 394. [CrossRef]
34. Shlesinger, M.F.; West, B.J.; Klafter, J. Levy dynamics of enhanced diffusion: Application to turbulence. *Phys. Rev. Lett.* **1987**, *58*, 1100. [CrossRef] [PubMed]
35. Richardson, L.F. Atmospheric diffusion shown on a distant-neighbour graph. *Proc. Roy. Soc.* **1926**, *110*, 709.
36. Kolmogorov, A.N. The local structure of turbulence in incompressible viscous fluid for very large Reynolds' numbers. *Doklady Akademii Nauk SSSR* **1941**, *30*, 301–305. (In Russian)
37. Korolev, V.Y.; Skvortsova, N.N. *Stochastic Models of Structural Plasma Turbulence*; Boston: Leiden, The Netherlands, 2006; 409p.
38. Gusakov, E.; Irzak, M.; Popov, A. Radial correlation reflectometry at oblique probing wave incidence (linear scattering theory predictions). *Plasma Phys. Control. Fusion* **2014**, *56*, 025009. [CrossRef]
39. Piliya, A.D.; Popov, A.Y. On application of the reciprocity theorem to calculation of a microwave radiation signal in inhomogeneous hot magnetized plasmas. *Plasma Phys. Control. Fusion* **2002**, *44*, 467. [CrossRef]
40. Urazbaev, A.O.; Vershkov, V.A.; Soldatov, S.V.; Shelukhin, D.A. Investigation of the possibility of using correlation reflectometry to determine the parameters of small-scale turbulence in the core of a tokamak plasma. *Plas. Phys. Rep.* **2006**, *32*, 443–460. [CrossRef]
41. Vershkov, V.A.; Soldatov, S.V.; Shelukhin, D.A. Dependence of Core Turbulence on the Discharge Parameters on T-10 and Its Correlation with Transport. In Proceedings of the 16th Fusion Energy Conference, Montreal, QC, Canada, 7–11 October 1996; Volume 1, pp. 519–533.
42. Vershkov, V.A.; Soldatov, S.V.; Dreval, V.V. A three-wave heterodyne correlation reflectometer developed in the T-10 tokamak. *Rev. Sci. Instrum.* **1999**, *70*, 1700. [CrossRef]

43. Osipenko, M.B.; T-10 Team. Transport and turbulence studies in the T-10 tokamak. *Nucl. Fusion* **2003**, *43*, 1641. [CrossRef]
44. Melnikov, A. Evolution of heavy ion beam probing from the origins to study of symmetric structures in fusion plasmas. *Symmetry* **2021**, *13*, 1367. [CrossRef]
45. Vershkov, V.A.; Buldakov, M.A.; Subbotin, G.F.; Shelukhin, D.A.; Melnikov, A.V.; Eliseev, L.G.; Karchev, N.K.; Khabanov, P.O.; Drabinskiy, M.A.; Sergeev, D.S. 3D structure of density fluctuations in the T-10 tokamak and new approach for current profile estimation. *Nucl. Fusion* **2019**, *59*, 066021. [CrossRef]
46. Landau, L.D.; Lifshitz, E.M.; Pitaevskii, L.P. *Electrodynamics of Continuous Media*; Butterworth-Heinemann: Oxford, UK, 1984; ISBN 978-0-7506-2634-7.
47. Bekefi, G. *Radiation Processes in Plasmas*; Wiley: New York, NY, USA, 1966; p. 377.
48. Kukushkin, A.B. Incoherent light scattering by a finite volume of a relativistic plasma. *Sov. J. Plasma Phys.* **1981**, *7*, 63.
49. Gusakov, E.Z.; Popov, A.Y. Non-linear theory of fluctuation reflectometry. *Plasma Phys. Control. Fusion* **2002**, *44*, 2327. [CrossRef]
50. Kramer-Flecken, A.; Dreval, V.; Soldatov, S.; Rogister, A.; Vershkov, V. Turbulence studies with means of reflectometry at TEXTOR. *Nucl. Fusion* **2004**, *44*, 1143–1157. [CrossRef]
51. Lechte, C.; Conway, G.D.; Gorler, T.; Troster-Schmid, C. X mode Doppler Reflectometry k-spectral measurements in ASDEX Upgrade: Experiments and simulations. *Plasma Phys. Control. Fusion* **2017**, *59*, 075006. [CrossRef]
52. Schirmer, J.; Conway, G.D.; Holzhauer, E.; Suttrop, W.; Zohm, H. Radial correlation length measurements on ASDEX Upgrade using correlation Doppler reflectometry. *Plasma Phys. Control. Fusion* **2007**, *49*, 1019–1039. [CrossRef]
53. Ivanov, V.V. $\epsilon\sqrt{}$ Law: Centennial of the First Exact Result of Classical Radiative Transfer Theory. In *Springer Series in Light Scattering*; Kokhanovsky, A., Ed.; Springer: Cham, Switzerland, 2021. [CrossRef]